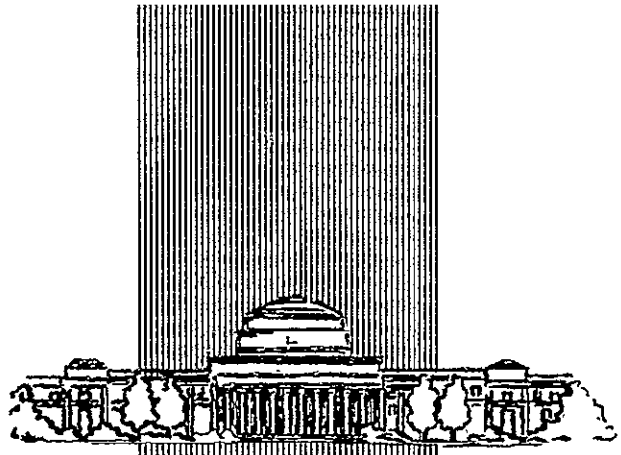

MASSACHUSETTS INSTITUTE OF TECHNOLOGY

OPTIMAL N-BURN MULTIORBIT INJECTION

by

Robert L. Singleton, Jr.

September 1971

Degree of Master of Science

T-554

PREPARED AT

CHARLES STARK DRAPER LABORATORY

CAMBRIDGE, MASSACHUSETTS, 02139

OPTIMAL N-BURN MULTIORBIT INJECTION

by

ROBERT L. SINGLETON, JR.
B. S. E., Princeton University
(1970)

SUBMITTED IN PARTIAL FULFILLMENT
OF THE REQUIREMENTS FOR THE
DEGREE OF MASTER OF SCIENCE
at the
MASSACHUSETTS INSTITUTE OF TECHNOLOGY
September, 1971

Signature of Author Robert L Singleton Jr
Department of Aeronautics
and Astronautics, June, 1971

Certified by Richard H. Battin
Thesis Supervisor

Certified by Theodore N. Edelbaum
Thesis Supervisor

Accepted by Sidney C. Beeny
Chairman, Departmental
Graduate Committee

ACKNOWLEDGMENTS

The author is indebted to Mr. T. N. Edelbaum for his motivation of the subject presented in this thesis and for his guidance and encouragement throughout its development. Acknowledgment is also made to Steve Croopnik for his administrative support and to Dr. Battin for his review of the final paper.

A special note of appreciation is extended to the Charles Stark Draper Laboratory for having provided its research facilities and to the National Science Foundation for having supported the author's graduate study at M. I. T.

This report was prepared under DSR Project 55-41200, sponsored by the Manned Spacecraft Center of the National Aeronautics and Space Administration through Contract NAS 9-10386.

The publication of this report does not constitute approval by the Charles Stark Draper Laboratory or the National Aeronautics and Space Administration of the findings or the conclusions contained herein. It is published only for the exchange and stimulation of ideas.

OPTIMAL N-BURN MULTIORBIT INJECTION

by

Robert L. Singleton, Jr.

Submitted to the Department of Aeronautics and Astronautics on June 21, 1971 in partial fulfillment of the requirements for the degree of Master of Science.

ABSTRACT

A method of minimizing gravity losses in orbital escape maneuvers, known as "perigee propulsion" or "multiorbit injection", has been found to have a useful application in transfer problems involving high specific-impulse powerplants such as nuclear rockets. Unlike conventional chemical rockets which typically have thrust phases that can be approximated by velocity impulses, new-generation powerplants require powered phases of finite duration to effect a required velocity change, and the impulsive approximation is no longer valid for evaluating the performance of the vehicle. A theory has recently been proposed, however, which establishes ground rules for computing characteristic velocity losses over an optimally-steered, finite-thrust trajectory on the basis of the velocity impulse required for the same maneuver. Utilizing this theory, this thesis develops a procedure for computing gravity losses over an N-burn multiorbit escape trajectory of specified

final energy and presents a technique which can be readily and efficiently employed to predict optimal burn schedules for time-open and time-fixed multiorbit escape maneuvers.

Thesis Supervisor: R. H. Battin, Sc. D.

Title: Associate Director, C. S. Draper Laboratory, M. I. T.

Thesis Supervisor: T. N. Edelbaum, M. S.

Title: Deputy Associate Director, C. S. Draper Laboratory, M. I. T.

TABLE OF CONTENTS

LIST OF SYMBOLS

Symbol	
$\underline{a}$	thrust acceleration vector
$\underline{a}_F$	finite thrust acceleration vector
c	exhaust velocity
$\underline{d}$	position discontinuity due to finite thrusting
f	moment correction factor
F	thrust magnitude
$\underline{g}$	gravity vector
G	gravity gradient matrix
i	subscript referring to beginning of burn segment
I_{sp}	specific impulse
J	augmented cost function
k	subscript referring to a particular burn segment
m	mass of vehicle
M_2	second moment of thrust about its centroid
N	number of burns
$\underline{r}$	position vector
R	radius of initial circular orbit
t	time
T	period of orbit
T_s	total transfer time
T_{sd}	desired transfer time
T_b	burn time

$\underline{v}$	velocity vector
V	absolute velocity
V_o	initial circular velocity
V_E	escape velocity
V_H	hyperbolic velocity
V_{H_P}	hyperbolic velocity at perigee
V_∞	excess hyperbolic velocity (final velocity)
$V\infty d$	desired final velocity
ΔV	velocity impulse variable
ΔV_I	characteristic velocity over an impulsive trajectory
ΔV_F	characteristic velocity over a finite-thrust trajectory
ΔV_G	generalized velocity impulse
ΔV^*	characteristic velocity loss
α	angle between thrust acceleration vector and primer vector
θ	angle between mean thrust direction and local horizontal
$\underline{\lambda}$	primer vector
$\lvert\underline{\lambda}\rvert$	primer vector magnitude
λ	Lagrange multiplier
$\underline{\mu}$	adjoint to position vector
μ	gravitational constant
ϕ	cost function

ψ	constraint
ν	Lagrange multiplier
ω_s	schuler frequency

CHAPTER I

INTRODUCTION

An interplanetary orbital transfer, such as injection from an orbit about the earth into a hyperbolic trajectory to Mars, can theoretically be effected without gravity losses by an impulsive velocity change at perigee. Using conventional chemical-fuel propulsion, the velocity change required by the transfer, i.e., the difference in periapsis velocity at the junction of the two orbits, can be achieved with a high-thrust burn, the duration of which is typically much less than the period of the initial orbit. Hence, for many orbital transfer problems, a single velocity impulse is very often a good approximation for the added velocity increment. The impulsive approximation is not valid, however, for vehicles requiring finite burns to effect a required velocity change, where, by "finite", it is presumed that the burn time is not negligible with respect to the period of the orbit and that the thrust segment is distributed over a significant portion of the flight path. Finite thrust characteristics must be taken into consideration in missions involving new-generation powerplants, such as solid-core nuclear rockets or electric propulsion devices. For example, a typical low-acceleration nuclear-powered injection maneuver using continuous thrusting would require a long, spiralling trajectory with much of the energy being applied in regions of low velocity.

A critical factor in the determination of the initial thrust-to-weight ratio is gravity losses, which are defined to be the

difference in the impulsive velocity change ΔV_I required for an injection maneuver of specified excess hyperbolic velocity V_∞ and the characteristic velocity ΔV_F required by the vehicle to perform a maneuver of the same magnitude using finite thrust. Gravity losses, therefore, are interchangeably referred to as characteristic velocity losses ΔV^*, given by

$$\Delta V^* = \Delta V_F - \Delta V_I \tag{1-1}$$

Energy addition efficiency is defined to be maximum for a given transfer when there are no characteristic velocity losses and when energy is applied in the region of highest velocity, as in the case of an impulsive transfer at perigee. Since the losses accumulated during high-thrust burns of short duration are very small, energy addition efficiency is near-optimal, and one-impulse transfers using conventional powerplants are a viable means of interplanetary maneuvering. For new generation powerplants requiring finite thrust, however, an alternate thrust program to minimize gravity losses must be proposed if such devices are to be applied economically and efficiently to interplanetary missions.

A thrust program which dramatically reduces gravity losses over finite-thrust transfers has been proposed under names such as "perigee propulsion" [9] and "multiorbit injection" [5]. These multiburn-multiorbit techniques maximize energy addition efficiency by applying thrust intermittently in regions of high

velocity (e. g., at perigee) and allowing the vehicle to coast under the influence of gravity between burns. The resulting flight path, shown in Figure 1, consists of a series of coaxial ellipses of sequentially increasing energy, along each of which the vehicle falls until it reaches the desired position with respect to the next perigee, where thrusting resumes and transfer to a higher orbit is effected.* When the vehicle arrives at perigee with sufficient energy to effect the required injection with a short burn, the multiorbit injection maneuver is complete.

The advantage of using the multiorbit technique for the injection maneuver is clear. Whereas a continuous thrust, spiralling trajectory typically requires initial thrust-to-weight ratios near 0.5, the multiorbit injection maneuver can make use of accelerations less than 0.1 g [9]. Furthermore, a specified payload can be powered by a smaller engine using a multiburn thrust schedule, or the payload for a given mission can be increased. This improvement in energy addition efficiency is gained, however, only at the expense of longer required transfer times. Nevertheless, for interplanetary missions requiring new generation powerplants, transfer times on the order of several days are still very small when compared to overall mission times measured in months or years.

The purpose of this study is to develop a simple method for arriving at the optimal multiorbit burn schedule for both

*Pericenter is not at the same position for each orbit as is implied in Figure 1. Each burn is accompanied by a small radial displacement as described in Chapter 2.

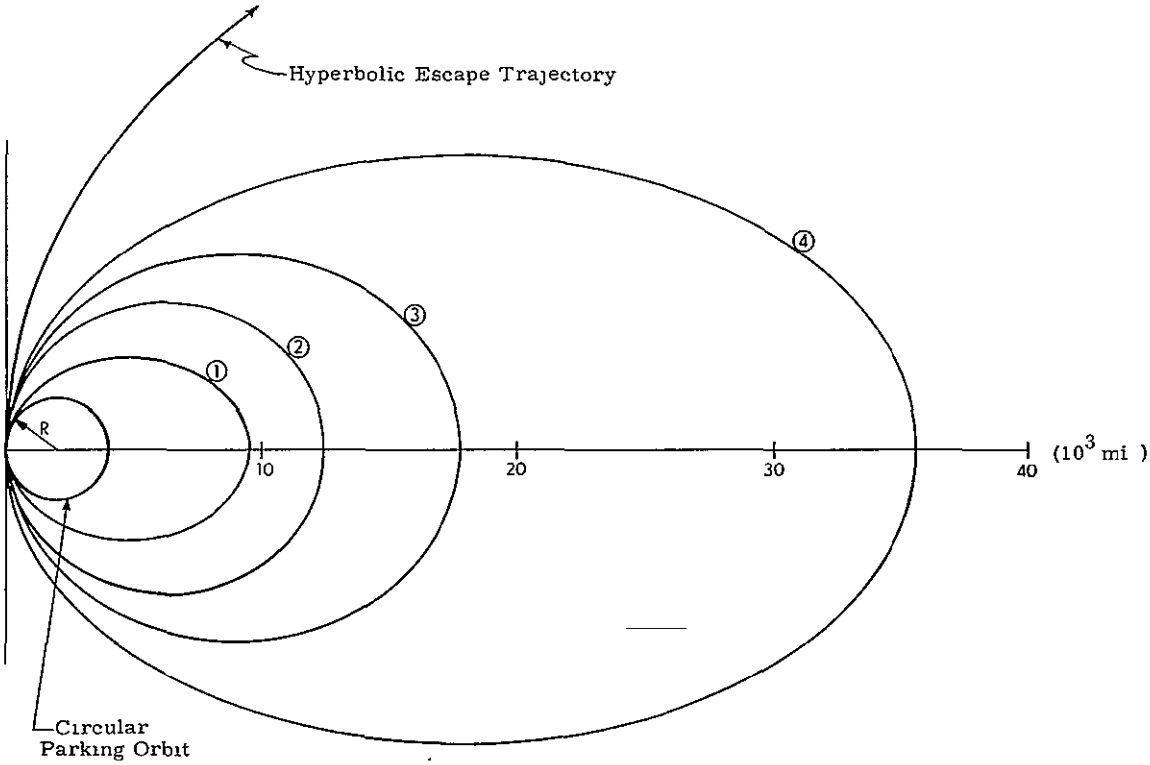

Figure 1.1 Five-Burn Multiorbit Injection

time-open and time-fixed injection maneuvers from a circular near-Earth parking orbit to a hyperbolic escape trajectory of specified excess hyperbolic velocity V_∞. The optimal burn schedule is defined to be that thrust program which minimizes the gravity losses for a multiorbit injection maneuver of a specified number of burns, subject to the initial orbital parameters, the final time and energy constraints, and the nature of the characteristic velocity approximation. In the following analysis, the effects of a third body will be ignored, and a simple planar model for an orbital transfer in an inverse-square central field will be utilized.

The following chapter will develop the equations used to calculate gravity losses over an N-burn multiorbit trajectory and will outline the assumptions required to permit a closed-form computational technique. Also included in Chapter 2 are the impulsive velocity and primer vector solutions for the injection maneuver. Chapter 3 contains a derivation of the approximate solution to the optimal time-open transfer and a presentation of an efficient algorithm for generating optimal N-burn trajectories for both time-open and time-fixed injection maneuvers. Chapter 4 presents a description of the procedure used and a summary of the results obtained for a typical multiburn injection maneuver. A set of conclusions are presented in Chapter 5. The Appendix contains a derivation of Robbins' "impulsive approximation", a listing of the orbital and powerplant data for a typical injection maneuver, and an outline of the computer simulations used in this study.

CHAPTER II

GRAVITY LOSSES ON A MULTIORBIT INJECTION MANEUVER

2.1 The "Impulsive Approximation" for the Characteristic Velocity

Earlier studies [5, 6, 9] have considered the multiorbit injection problem and have computed characteristic velocity losses using non-optimal steering criteria and numerical integration over the thrust trajectory. This analysis, however, will develop a procedure to obtain the optimal N-burn thrust program which incorporates not only optimal steering but also a convenient and simple closed-form method for calculating gravity losses. The groundwork for this analysis has been laid out in a report by H. Robbins [12], in which a method is presented for predicting characteristic velocity losses over a finite-thrust trajectory on the basis of the velocity impulse required to effect the equivalent maneuver. Robbins' approximation is derived in Appendix A.

The result of Robbins' approximation, as derived in the Appendix, expresses the characteristic velocity loss ΔV^* over a segmented finite-thrust trajectory in terms of the primer vector solution and the velocity impulses over the equivalent impulsive trajectory. The steering is assumed to vary linearly over each burn, and the centroid time for each burn corresponds to the time of occurrence of the equivalent velocity impulse. The result is given by

$$\Delta V^* = \frac{1}{2} \sum_{k=1}^{n} \left(-\underline{\lambda} \cdot G\,\underline{\lambda} - |\dot{\underline{\lambda}}|^2\right) M_{2_k} \qquad (2.1\text{-}1)$$

where $\underline{\lambda}$ is the primer vector of Lawden [10], M_{2_k} is the second moment of thrust about its centroid, and n is the number of burns. The second moment can be calculated from the expression

$$M_{2_k} = \frac{1}{12} \Delta V_{I_k} T_{b_k}^2 \qquad (2.1\text{-}2)$$

where ΔV_{I_k} is the equivalent velocity impulse on the k th burn and T_{b_k} is the duration of the k th burn. (2.1-2) is exact for constant thrust over the burn segment; however, to account for non-constant acceleration during the burn, the above equation can be multiplied by the correction factor f, which for the k th burn is given by

$$f_k = \frac{6c}{\Delta V_{I_k}} \left[\frac{-2c}{\Delta V_{I_k}} + \coth\left(\frac{\Delta V_{I_k}}{2c}\right)\right]$$

$$= 1 - \frac{1}{60}\left(\frac{c}{\Delta V_{I_k}}\right)^2 + \frac{1}{1920}\left(\frac{c}{\Delta V_{I_k}}\right)^4 + \ldots \qquad (2.1\text{-}3)$$

where c is the exhaust velocity.

Although the characteristic velocity on the k th burn is calculated as a function of the equivalent velocity impulse ΔV_{I_k} for that burn, it is important to note that the k th finite-thrust segment is actually centered about a generalized velocity

impulse ΔV_{G_k}, which has position discontinuities $\underline{d}_k$ at the impulse times t_k given by

$$\underline{d}_k = - \dot{\underline{\lambda}} (t_k) \, M_{2_k} \tag{2.1-4}$$

and which differs in magnitude from ΔV_{I_k} as follows:

$$\Delta V_{G_k} - \Delta V_{I_k} = \dot{\underline{\lambda}} (t_k) \cdot \underline{d}_k = - \left| \dot{\underline{\lambda}} (t_k) \right|^2 M_{2_k} \tag{2.1-5}$$

Since $\underline{\lambda} (t_k)$ is perpendicular to $\underline{\lambda} (t_k)$, the position discontinuity is radial at each perigee burn and its magnitude is of the order of $|\underline{\lambda} (t_k)|$. Thus, the displacement of one perigee with respect to another on an optimally steered and timed multiorbit trajectory is small enough with respect to the semimajor axis of the orbit to be neglected.

It can be shown that the first term in parentheses on the right hand side of (2.1-1) is equivalent to the gravity gradient $-g_{xx}$, where x is the mean direction of thrust acceleration, that is, along $\underline{\lambda} (t_k)$. The second term, $|\dot{\underline{\lambda}}|^2$, is equal to the square of the optimal turning rate of the thrust vector. For short burns, a constant average value for g_{xx} is a good approximation; and, for the simple orbital model described, this term is given by

$$-g_{xx} = \frac{\mu}{r^3} (1 - 3 \sin^2 \theta) \tag{2.1-6}$$

where μ is the gravitational constant, r is the distance from the center of attraction, and θ is the angle between the mean thrust direction and the local horizontal. Therefore, for a n-burn multiorbit trajectory in a planar, inverse-square central field, Robbins' approximation yields the following equation for computing the characteristic velocity loss:

$$\Delta V^* = \frac{1}{24} \sum_{k=1}^{n} \left[\frac{\mu}{r^3} (1 - 3 \sin^2 \theta) - \left| \dot{\underline{\lambda}} \right|^2 \right] \Delta V_{I_k} \; f_k \; T_{b_k}^{\;2} \tag{2.1-7}$$

2.2 Thrust and Orbital Constraints

The multiorbit injection maneuver considered in this study consists of an N-burn transfer from a circular orbit of radius R (close to the earth) to a hyperbolic escape trajectory with specified V_∞. The transfer profile describes a series of (N-1) intermediate elliptical coasting orbits between the initial and final burns. The transfer time T_s is equal to the sum of the periods of the (N-1) coasting orbits. Each perigee burn is executed such that its centroid occurs at the junction of the circular orbit and the (approximately equal) perigees of the N succeeding conic orbits, and the thrust acceleration vector is applied parallel to the primer vector, such that optimal timing and steering requirements, respectively, are satisfied.

Having specified N, R, and V_∞, sufficient information is available to compute the characteristic velocity loss for a multi-orbit escape maneuver from an Earth orbit. Certain constraints must be imposed on the analysis, however, to assure validity of Robbins' approximation and a closed-form calculation of the performance penalty. First, r and θ are assumed to remain constant over each burn. This assumption places no further restrictions on the problem, since it is consistent with Robbins' short burn criterion. Therefore, assuming that the position discontinuities $\underline{d}_k$ are much smaller than the radius of the initial orbit, and specifying $r = R$ and $\theta = 0$ for each perigee burn, the characteristic velocity loss for an N-burn multiorbit injection maneuver is given by

$$\Delta V^* = \frac{1}{24} \sum_{k=1}^{N} \left(\frac{u}{R^3} - \left| \dot{\underline{\lambda}} \right|^2 \right) \Delta V_{I_k} \, f_k \, T_{b_k}^{\,2} \qquad (2.2\text{-}1)$$

Exactly what is meant by a "short" burn in the analytical sense is not given in [12]. However, Robbins' analysis demonstrates that, in order for a burn to be short, the dimensionless quantity $\omega_s \, T_{b_k}$ must be sufficiently small, where ω_s, the Schuler Frequency is defined as

$$\omega_s = \sqrt{\frac{\mu}{r^3}} \qquad (2.2\text{-}2)$$

Furthermore, by a rough analysis, Robbins finds that the short burn approximation is quite good for values of $\omega_s \, T_{b_k}$ as large as

unity and progressively worse for values beyond this arbitrary value. One indication of the range of flexibility offered by this semi-arbitrary short-burn constraint is the maximum allowable burn time permitted by it. Comparing the maximum burn time given by

$$T_{b\ max} = \frac{1}{\omega_s} = \sqrt{\frac{r^3}{\mu}} \qquad (2.2\text{-}3)$$

with the period of the circular orbit,

$$T_o = 2\pi\sqrt{\frac{r^3}{\mu}}$$

The following limit is obtained for a short burn:

$$T_{b_k} < \frac{T_o}{2\pi} \sim .16\ T_o \qquad (2.2\text{-}4)$$

In other words, using the short burn criterion based on ω_s, Robbins' approximation is valid on thrust trajectories over arcs up to a magnitude equivalent in time to a trajectory covering 16% of the circular orbit. This result is rather optimistic, if not surprising. Nonetheless, Robbins' short burn criterion has been shown to give accurate results and will be used as an upper limit in the optimal N-burn multiorbit injection analysis.

For a time-open transfer, that is, one for which the total time between the initial and final burns is unspecified, the orbital

constraints are the requirements that (1) the velocity after the last burn will satisfy the final energy constraint and (2) the velocity on the next-to-last burn (k = N - 1) will be less than the escape velocity, given by

$$V_E = \sqrt{2}\, V_o \qquad (2.2\text{-}5)$$

where V_o is the velocity of the vehicle in circular parking orbit given by

$$V_o = \sqrt{\frac{\mu}{R}} \qquad (2.2\text{-}6)$$

The first requirement will be described in the next section. The latter criterion is necessary to constrain to transfer to the specified number of burns N.

2.3 The Velocity Impulse and Primer Vector Solutions

For an impulsive transfer from a circular orbit to a hyperbolic trajectory, the required velocity impulse ΔV_I is equal to the difference in the periapsis velocity of the hyperbolic trajectory V_{H_P} and the initial circular velocity V_o. The energy equation for a hyperbolic orbit is given by

$$V_H^2 = \mu\left(\frac{2}{r} + \frac{1}{a}\right) \qquad (2.3\text{-}1)$$

where a, the semimajor axis is taken to be negative. If the escape velocity at infinity ($r \rightarrow \infty$) is specified to be V_∞, a is determined uniquely, and the hyperbolic velocity at perigee ($r = R$) is given by

$$V_{H_P} = \sqrt{\frac{2\mu}{R} + V_\infty^2} \qquad (2.3\text{-}2)$$

or

$$V_{H_P} = \sqrt{V_E^2 + V_\infty^2} \qquad (2.3\text{-}3)$$

The total required impulsive velocity can then be written as

$$\begin{aligned} \Delta V_I &= V_{H_P} - V_o \\ &= \sqrt{V_E^2 + V_\infty^2} - V_o \end{aligned} \qquad (2.3\text{-}4)$$

The primer vector solution for this transfer can be obtained in a simple manner from an examination of the necessary conditions along an optimal thrust trajectory. In order for energy addition efficiency to be maximized along an impulsive trajectory, the velocity impulse must occur at a local maximum of the primer vector time history, and, immediately after the impulse, necessary conditions for the trajectory to be optimal are given by the relations [10]

$$\begin{aligned} \underline{\lambda} &\propto \underline{v} \\ \dot{\underline{\lambda}} &\propto \underline{g} \end{aligned} \qquad (2.3\text{-}5)$$

where, immediately after the impulse, the magnitude of the gravity vector is (μ/R^2) and the velocity is the periapsis velocity of the hyperbola V_{H_P}. From the conditions given by (2.3-5), the following relationship can be written:

$$\frac{\dot{\underline{\lambda}}}{\underline{\lambda}} = \frac{\underline{g}}{\underline{v}} \tag{2.3-6}$$

Thus, since the magnitude of the primer vector immediately after the impulse is defined to be unity along an optimal trajectory, (2.3-6) can be written as

$$\left|\dot{\underline{\lambda}}\right| = \frac{\mu}{R^2 V_{H_P}} \tag{2.3-7}$$

and the primer vector solution to be used in the calculation of the performance penalty (2.2-1) is given by

$$\left|\dot{\underline{\lambda}}\right|^2 = \frac{\mu^2}{R^4\left(V_\infty^{\,2} + V_E^{\,2}\right)} \tag{2.3-8}$$

CHAPTER III

OPTIMAL N-BURN THRUST PROGRAMS

3.1 Approximate Time-Open Solution

The optimal burn schedule for the time-open multiorbit injection maneuver is that thrust program which, subject to the appropriate constraints, minimizes the characteristic velocity loss over the entire trajectory. Using the primer vector solution obtained in Section 2.3, the characteristic velocity loss given by (2.2-1) can be rewritten as

$$\Delta V^* = \frac{1}{24} \sum_{k=1}^{N} \left[\frac{\mu}{R^3} - \frac{\mu^2}{R^4 \left(V_\infty^2 + V_E^2 \right)} \right] \Delta V_{I_k} f_k T_{b_k}^2 \tag{3.1-1}$$

which can be reduced to

$$\Delta V^* = C_\infty \sum_{k=1}^{N} \Delta V_{I_k} f_k T_{b_k}^2 \tag{3.1-2}$$

where the constant C_∞, specified by the transfer constraints, is given by

$$C_\infty = \frac{\mu}{24 R^3} \left(\frac{V_\infty^2 R + \mu}{V_\infty^2 R + 2\mu} \right) \tag{3.1-3}$$

For a single burn, the burn time T_b for a constant thrust powerplant can be expressed in terms of the equivalent velocity

change ΔV over the burn segment, i. e.,

$$T_b = \frac{m_o c}{F}\left(1-e^{-\frac{\Delta V}{c}}\right) \tag{3.1-4}$$

where m_o is the initial mass of the vehicle, c is the exhaust velocity, and F is the thrust magnitude. For a multiorbit-multiburn trajectory, the burn time for the kth powered phase can be expressed by taking the difference in the burn time before and after the burn. If T_{b_i} and $T_{b_{i+1}}$ are defined to be the times at the beginning and end, respectively, of the kth powered phase (i = k), and if ΔV_i and ΔV_{i+1} are the corresponding values of the total impulse up to times T_{b_i} and $T_{b_{i+1}}$, respectively, then the velocity increment ΔV_{I_k} on the kth burn segment is given by

$$\Delta V_{I_k} = \Delta V_{i+1} - \Delta V_i \tag{3.1-5}$$

The burn time on the kth segment is then given by

$$T_{b_k} = T_{b_{i+1}} - T_{b_i} = \frac{m_o c}{F}\left(e^{-\frac{\Delta V_i}{c}} - e^{-\frac{\Delta V_{i+1}}{c}}\right)$$

or,

$$T_{b_k} = \frac{m_o c}{F} e^{-\frac{\Delta V_i}{c}}\left(1 - e^{-\frac{\Delta V_{I_K}}{c}}\right) \tag{3.1-6}$$

Defining the mass at time T_{b_i} to be

$$m_i = m_o e^{\frac{-\Delta V_i}{c}} \tag{3.1-7}$$

the kth burn time can be written as

$$T_{b_k} = \frac{m_i}{F} c \left(1 - e^{\frac{-\Delta V_{I_k}}{c}}\right) \tag{3.1-8}$$

It is now clear that, since T_{b_k} can be expressed in terms of the equivalent velocity impulse on the kth segment ΔV_{I_k}, the optimal burn schedule, $T_{b_1}, T_{b_2}, \ldots T_{b_N}$, can be obtained from the velocity impulse schedule, $\Delta V_{I_1}, \Delta V_{I_2}, \ldots \Delta V_{I_N}$, which minimizes the characteristic velocity loss (3.1-2).

The optimal N-burn time-open burn schedule can be found by performing a parameter optimization on the impulse schedule and satisfying the appropriate constraints. For a specified V_∞, the sum of the N velocity impulses must equal the total required impulse ΔV_I given by (2.3-4). Furthermore, each burn must be "short", and the periapsis velocity after the next-to-last burn must be less than the escape velocity, as described in 2.2. Therefore, the time-open multiorbit parameter optimization problem for specified N and V_∞ can be expressed as follows:

$$\text{Minimize: } \phi = C_\infty \sum_{k=1}^{N} \Delta V_{I_k} f_k T_{b_k}^2 \tag{3.1-9}$$

Subject to:

$$1) \quad \sum_{k=1}^{N} \Delta V_{I_k} = \Delta V_I = \sqrt{V_E^2 - V_\infty^2} - V_o \qquad (3.1\text{-}10)$$

$$2) \quad T_{b_k} < T_{b_{max}} = \sqrt{\frac{R^3}{\mu}} \qquad (3.1\text{-}11)$$

$$3) \quad V_{N-1} < V_E \qquad (3.1\text{-}12)$$

where ϕ defines the cost function ΔV^* and V_{N-1} corresponds to the absolute periapsis velocity after the N-1st burn.

The number of burns is not taken as a parameter in the above formulation, since ϕ is not differentiable with respect to N. It can be seen that the cost function for the time-open maneuver is a minimum for a burn schedule consisting of N infinitely small impulses, which correspond to an infinitely large number of burns. However, the short burn and velocity constraints put an upper limit on the number of burns for a given V_∞. Nevertheless, if V_∞ is small $(V_\infty \rightarrow 0)$, N will get very large, and the solution is clearly impractical. Therefore, the optimal time-open solution would have to be chosen on the basis of a transfer-time/performance-penalty tradeoff between solutions corresponding to various values for N.

An approximate solution for the optimal time-open burn schedule can be obtained by assuming that the mass decrease

over each burn is negligible (e. g., for high exhaust velocity powerplants). The burn time for each segment is then given by

$$T_{b_k} \approx \frac{m_o c}{F}\left(1 - e^{\frac{-\Delta V_{I_k}}{c}}\right) \qquad (3.1\text{-}13)$$

As a simple case, consider the two-burn transfer for which the cost function can be written as

$$\phi_2 = C_\infty \left(\Delta V_{I_1} f_1 T_{b_1}{}^2 + \Delta V_{I_2} f_2 T_{b_2}{}^2\right) \qquad (3.1\text{-}14)$$

Assuming that the inequality constraints (3.1-11, 12) are satisfied, the minimization of ϕ_2 is subject only to the velocity constraint (3.1-10) given by

$$\psi_2 = \Delta V_I - \left(\Delta V_{I_1} + \Delta V_{I_2}\right) = 0 \qquad (3.1\text{-}15)$$

The solution to this simple two-parameter minimization problem can be obtained by defining the Lagrange multiplier ν as a penalty on the constraint and by solving the Euler-Lagrange equations which describe the necessary condition for a stationary point, i. e.,

$$\frac{\partial (\phi + \nu \psi)}{\partial \Delta V_{I_i}} = 0 \quad (i = 1, 2, \ldots N) \qquad (3.1\text{-}16)$$

Assuming that $f_k = 1$ for all values of k (which is a very good

approximation), the required partials of (3.1-16) can be computed to give

$$\left(\frac{m_o c}{F}\right)^2 \left(1-e^{\frac{-\Delta V_{I_1}}{c}}\right)^2 + \frac{2 m_o}{F} \Delta V_{I_1} e^{\frac{-\Delta V_{I_1}}{c}} \left(1-e^{\frac{-\Delta V_{I_1}}{c}}\right) + \frac{\nu}{C_\infty} = 0$$

$$\left(\frac{m_o c}{F}\right)^2 \left(1-e^{\frac{-\Delta V_{I_2}}{c}}\right)^2 + \frac{2 m_o}{F} \Delta V_{I_2} e^{\frac{-\Delta V_{I_2}}{c}} \left(1-e^{\frac{-\Delta V_{I_2}}{c}}\right) + \frac{\nu}{C_\infty} = 0 \qquad (3.1\text{-}17)$$

Equating the expressions for ν/C_∞ given by (3.1-17), the obvious result is the relation

$$\Delta V_{I_1} = \Delta V_{I_2} \qquad (3.1\text{-}18)$$

$$T_{b_1} = T_{b_2} \qquad (3.1\text{-}19)$$

In other words, the approximate two-burn, time-open optimal burn schedule is characterized by burns of equal magnitude and duration.

Since the moment correction factor f_k on the kth burn is a function of the kth velocity impulse ΔV_{I_k}, removing the assumption that $f_k = 1$ does not change the above result. Moreover, this result can be extended to the general N-burn time-open transfer. With the same initial assumptions used for the two-burn maneuver,

the N-burn optimization problem can be written as follows:

$$\min: \ \phi = \sum_{k=1}^{N} \Delta V_{I_k} \dot{F}_k T_{b_k}^2$$

$$\text{Subject to:} \quad \psi = \Delta V_I - \sum_{k=1}^{N} \Delta V_{I_k} = 0 \tag{3.1-20}$$

The necessary conditions for a stationary point are given by

$$\frac{\partial \phi}{\partial \Delta V_{I_1}} + \frac{\nu \partial \psi}{\partial \Delta V_{I_1}} = 0$$

$$\frac{\partial \phi}{\partial \Delta V_{I_2}} + \frac{\nu \partial \psi}{\partial \Delta V_{I_2}} = 0 \tag{3.1-21}$$

$$\vdots \qquad \vdots \qquad \vdots$$

$$\frac{\partial \phi}{\partial \Delta V_{I_N}} + \frac{\nu \partial \psi}{\partial \Delta V_{I_N}} = 0$$

where, without further manipulation, the solution is clearly given by equal velocity impulses and equal burn times:

$$\Delta V_{I_k} = \frac{\Delta V_I}{N}$$

$$T_{b_k} = \frac{m_o c}{F}\left(1 - e^{\frac{-\Delta V_I}{NC}}\right) \qquad k = 0, 1, 2, \ldots N \tag{3.1-22}$$

The general result can be stated as follows: For an N-burn, time-open multiorbit transfer for which the mass decrease over each thrust phase is negligible, the optimum burn schedule is prescribed by specifying each perigee burn to be of equal duration. This result is conditioned, of course, on the satisfaction of the inequality constraints. Hence, for a given V_∞, a lower limit on the number of burns is established by the short-burn constraint (3.1-11), and an upper limit is placed on N by the escape velocity constraint (3.1-12).

These results are summarized for a typical injection maneuver in Figures 3.1 and 3.2. The approximate time-open simulation is described in Appendix C.1; the orbital parameters and power plant data used in all the simulations are listed in Appendix B. The vehicle selected for this study is a nuclear solid-core rocket with a capability consistent with the technology for the late 1970's or early 1980's; it has been assigned a thrust to weight ratio of 0.1 and a specific impulse of 800 seconds. Figure 3.1 shows the characteristic velocity loss ΔV^* as a function of the number of burns N for four different values of V_∞. The endpoints for each family of solutions are specified by the short burn and escape velocity constraints as described previously. Figure 3.2 illustrates the transfer time T_s as a function of N for the same values of V_∞. It is interesting to note that, as the upper limit on N is approached for a given V_∞, the time in orbit asymptotically approaches infinity. The limiting case for each value of

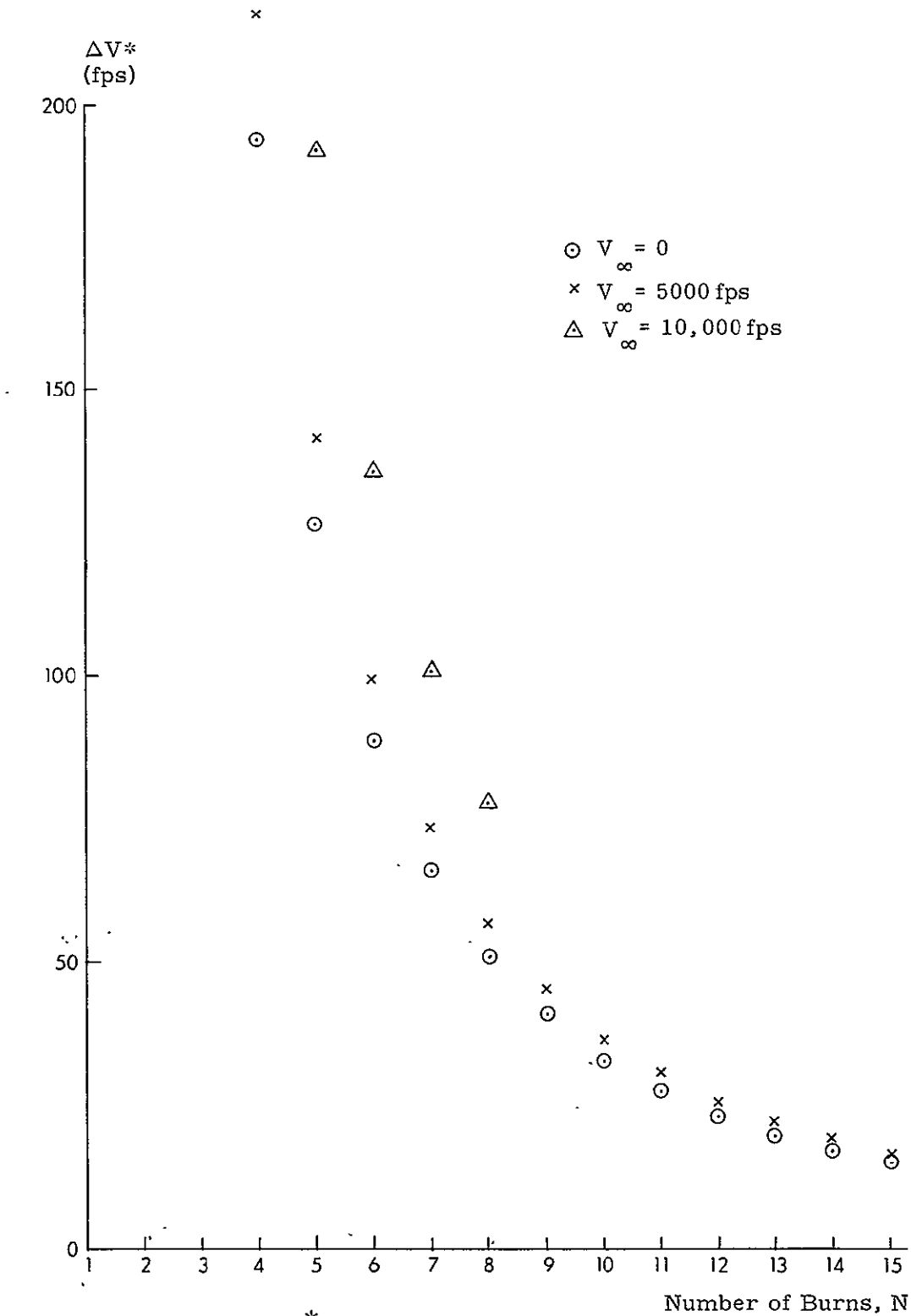

Figure 3.1 ΔV^* vs N For Approximate Time-Open Solution

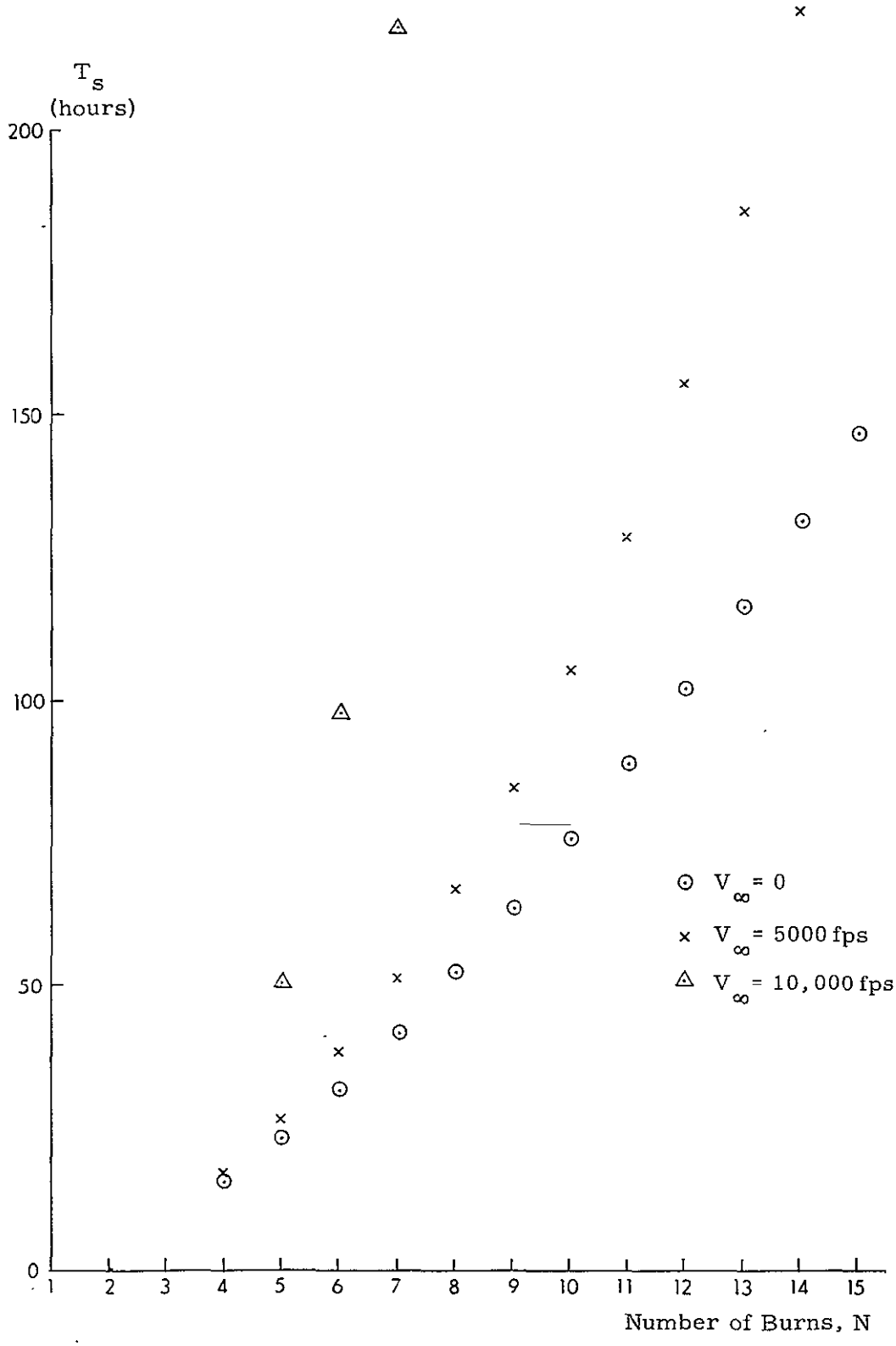

Figure 3.2 T_s vs N For Approximate Time-Open Solution

V_∞ corresponds to an (N-1)-burn parabolic escape for which the time in orbit is given by the lower family of solutions corresponding to $V_\infty = 0$. The limits on N for each value of V_∞ are listed in Table 3.1.

Table 3.1

Limits on N for the Approximate

Time-Open Optimal Transfer

(F/W = 0.1, I_{sp} = 800 sec.)

	Lower Limit	Upper Limit
V_∞ (fps)	$T_{b_k} > T_{b\,max}$	$V_{N-1} > V_E$
0	4	∞
5,000	4	31
10,000	5	8
15,000	-	-

An upper limit on V_∞ is specified by the short burn constraint. This fact accounts for the null solution corresponding to V_∞ = 15,000 fps in Table 3.1. For the approximate time-open solution, the upper limit on the excess hyperbolic velocity is

given by

$$V_{\infty\,max} = \sqrt{V_{H_{p\,max}} - V_E^2}$$

$$= \sqrt{\left(V_E + \Delta V_{I\,max}\right) - V_E^2} \qquad (3.1\text{-}23)$$

where, from (3.1-8), the maximum allowable velocity impulse $\Delta V_{I\,max}$ is given by

$$\Delta V_{I\,max} = -c\,\ell n\left(1 - \frac{T_{b\,max}\,F}{m_o\,c}\right)$$

$$= -c\,\ell n\left(1 - \frac{F}{m_o\,c}\sqrt{\frac{R^3}{\mu}}\right) \qquad (3.1\text{-}24)$$

For the maneuver simulated, these values are as follows:

$$T_{b\,max} = 837 \text{ sec.}$$

$$\Delta V_{I_{k\,max}} = 2,846 \text{ fps.}$$

$$V_{\infty\,max} = 14,640 \text{ fps.}$$

These results, as well as those obtained for the limits on N, imply that the upper family of solutions shown in Figures 3.1 and 3.2 are invalid, and demonstrate that the short burn constraint

is somewhat restrictive in terms of final obtainable energy.

Since the mass-loss approximation used in the above analysis rarely applies to typical propulsion systems, the approximate time-open solution is of little practical value. Nevertheless, the results are meaningful in the sense that they provide a simple heuristic framework from which to analyze the effects of and the restrictions imposed by velocity and burn time constraints on the optimal N-burn multiorbit maneuver.

3.2 Optimal Time-Open/Time-Fixed Solution

Consider the N-burn multiorbit injection maneuver for which the total transfer time is specified, that is, the time between the initiation of the first burn, which takes the vehicle out of parking orbit, and the escape burn, which occurs at the completion of the last intermediate coasting orbit, it assigned a particular value. Considering only the time constraint, the minimization problem can be stated as follows:

$$\min \phi = C_\infty \sum_{k=1}^{N} \Delta V_{I_k} f_k T_{b_k}^2 \qquad (3.2\text{-}1)$$

subject to:

$$\psi_1 = T_s - T_{sd} = 0 \qquad (3.2\text{-}2)$$

where T_{sd} is the specified, or desired, transfer time and T_s is

the actual transfer time, which is equal to the sum of the periods of the (N-1) intermediate orbits. The above problem can be restated as an unconstrained problem by defining the augmented cost function J such that

$$J = \phi + \nu_1 \psi_1 \qquad (3.2\text{-}3)$$

where ν_1 is a Lagrange multiplier which assigns a penalty to the unconstrained cost ϕ proportional to the deviation of the actual time T_s from the desired time T_{sd}. Hence, if $\nu_1 = 0$, the augmented cost J equals the unconstrained cost ϕ, and the minimization corresponds to the time-open maneuver.

The optimal burn schedule for the time-fixed maneuver could be obtained by means of a conventional constrained parameter optimization algorithm, such as a gradient projection scheme. An alternate, simpler approach will be considered here. The major advantage of the method to be derived is a reduction in the dimension of the problem to a form which lends itself to simple iterative methods. For purposes of simplification, the inequality constraints described in the previous section will be temporarily ignored.

First, let the variable ΔV_i be the total velocity impulse effected up to the total burn time T_{b_i}, which for constant

thrusting is given by

$$T_{b_i} = \frac{m_o c}{F}\left(1-e^{\frac{-\Delta V_i}{c}}\right) \qquad (3.2\text{-}4)$$

Recall the segment variables for the kth thrust phase previously defined as

$$\Delta V_{I_k} = \Delta V_{i+1} - \Delta V_i$$

$$T_{b_k} = T_{b_{i+1}} - T_{b_i} \qquad (3.2\text{-}5)$$

where k varies from 1 to N. The problem can now be restated in terms of the variables ΔV_i and T_{b_i}, which behave as continuous variables over the total burn interval of a multiburn-multiorbit trajectory. The characteristic velocity loss can be rewritten as

$$\Delta V^* = C_\infty \sum_{i=o}^{N-1} \left(\Delta V_{i+1} - \Delta V_i\right) f_k \left(T_{b_{i+1}} - T_{b_i}\right)^2 \qquad (3.2\text{-}6)$$

where f_k is a function of the quantity $\left(\Delta V_{i+1} - \Delta V_i\right)$. The total time in orbit is related to the variable ΔV_i by

$$T_s = \sum_{i=1}^{N-1} T_i\left(\Delta V_i\right) = \sum_{i=1}^{N-1} 2\pi\mu \left[\frac{R}{2\mu - R\left(V_o + \Delta V_i\right)^2}\right]^{3/2} \qquad (3.2\text{-}7)$$

where T_i is the period of the orbit following the ith burn.

The necessary condition for a stationary point of the augmented cost function J is given by

$$\frac{\partial J}{\partial \Delta V_i} = \frac{\partial \left(\phi + \nu_1 \psi_1 \right)}{\partial \Delta V_i} = 0 \qquad (3.2\text{-}8)$$

Assuming that $f_k = 1$ and taking the required partials of ΔV^* given by (3.2-6), the necessary condition becomes

$$C_\infty \left[-T_{b_k}{}^2 + T_{b_{k-1}}{}^2 + 2 \Delta V_{I_k} T_{b_k} \frac{\partial T_{b_k}}{\partial \Delta V_i} + 2 \Delta V_{I_{k-1}} T_{b_{k-1}} \frac{\partial T_{b_{k-1}}}{\partial \Delta V_i} \right] + \nu_1 \frac{\partial T_s \left(\Delta V_i \right)}{\partial \Delta V_i} = 0 \qquad (3.2\text{-}9)$$

where the k subscripts denote the segment quantities defined by (3.2-5). Utilizing (3.1-6), the required partials of the segment burn times are found to be

$$\frac{\partial T_{b_k}}{\partial \Delta V_i} = \frac{-m_o}{F} e^{\frac{-\Delta V_i}{c}} = \frac{-m_i}{F}$$

$$\frac{\partial T_{b_{k-1}}}{\partial \Delta V_i} = \frac{m_o}{F} e^{\frac{-\Delta V_i}{c}} = \frac{m_i}{F} \qquad (3.2\text{-}10)$$

If the quantity Q_k is defined, where

$$Q_k = \left(1 - e^{\frac{-\Delta V_{I_k}}{c}} \right) \qquad (3.2\text{-}11)$$

(3.2-9) can be written as

$$-c^2\left(\frac{m_i}{F}\right)^2 Q_k{}^2 + c^2\left(\frac{m_{i-1}}{F}\right)^2 Q_{k-1}{}^2 - 2c\left(\frac{m_i}{F}\right)^2 Q_k \Delta V_{I_k}$$

$$+ 2c\left(\frac{m_{i-1}}{F}\right)\left(\frac{m_i}{F}\right) Q_{k-1} \Delta V_{I_{k-1}} + \frac{\nu_1}{C_\infty} \frac{\partial T_s\left(\Delta V_i\right)}{\partial \Delta V_i} = 0 \qquad (3.2\text{-}12)$$

Rearranging, (3.2-12) can be reduced to

$$-\left(\frac{m_i}{F}\right)^2 Q_k \left(cQ_k + 2\Delta V_{I_k}\right) + 2\left(\frac{m_{i-1}}{F}\right)\left(\frac{m_i}{F}\right) Q_{k-1} \Delta V_{I_{k-1}}$$

$$+ \left(\frac{m_{i-1}}{F}\right)^2 c\, Q_{k-1}{}^2 + \frac{\nu_1}{C_\infty c} \frac{\partial T_s\left(\Delta V_i\right)}{\partial \Delta V_i} = 0 \qquad (3.2\text{-}13)$$

The variables ΔV_i corresponding to the optimal burn schedule must satisfy (3.2-13). The optimal burn schedule could be obtained by simultaneously satisfying (N-1) equations of the form (3.2-13) and the velocity constraint on the last burn given by

$$V_o + \Delta V_N = V_{H_P} = \sqrt{V_E{}^2 + V_\infty{}^2}$$

or,

$$\Delta V_N = \sqrt{V_E{}^2 + V_\infty{}^2} - V_o = \Delta V_I \qquad (3.2\text{-}14)$$

A simpler method for obtaining the optimal N-burn thrust program can be arrived at as follows: First, expand the kth

burn time given by (3.1-6) in a Taylor series about ΔV_i. To first order, this expansion is given by

$$T_{b_{i+1}} = f\left(\Delta V_i + \Delta V_{I_k}\right) \approx f\left(\Delta V_i\right) + \Delta V_{I_k} f'\left(\Delta V_i\right)$$

or,
$$T_{b_{i+1}} \approx T_{b_i} + \left(\Delta V_{i+1} - \Delta V_i\right) \frac{m_o}{F} e^{\frac{-\Delta V_i}{c}} \qquad (3.2\text{-}15)$$

Hence, the duration of the kth burn is approximated to first order by

$$T_{b_{i+1}} - T_{b_i} \approx \frac{m_i}{F}\left(\Delta V_{i+1} - \Delta V_i\right)$$

which, in terms of segment quantities, is given by

$$T_{b_k} \approx \frac{m_i}{F} \overline{\Delta V_{I_k}} \qquad (3.2\text{-}16)$$

Substituting this approximation for the burn time into (3.2-9), the first order necessary condition reduces to

$$-3\left(\frac{m_i}{F}\right)^2 \Delta V_{I_k}{}^2 + \left(\frac{m_{i-1}}{F}\right)^2 \Delta V_{I_{k-1}}{}^2 - 2\left(\frac{m_i}{F}\right)\left(\frac{m_{i-1}}{F}\right) \Delta V_{I_{k-1}}{}^2 + \frac{\nu_1}{C_\infty} \frac{\partial T_s\left(\Delta V_i\right)}{\partial \Delta V_i} = 0 \qquad (3.2\text{-}17)$$

Solving for $\Delta V_{I_k}^2$, the above equation becomes

$$\Delta V_{I_k}^2 = \frac{1}{3}\left[\left(\frac{m_{i-1}}{m_i}\right)^2 + 2\left(\frac{m_{i-1}}{m_i}\right)\right]\Delta V_{I_{k-1}}^2 + \frac{\nu_1}{3C_\infty}\left(\frac{F}{m_i}\right)^2 \frac{\partial T_s\left(\Delta V_i\right)}{\partial \Delta V_i} \tag{3.2-18}$$

Recalling the definition of ΔV_{I_k} given by (3.2-5), (3.2-18) can be utilized to give an expression for the total velocity impulse ΔV_{i+1} at the end of the kth burn as follows:

$$\Delta V_{i+1} = \Delta V_i + \sqrt{\frac{1}{3}\left[\left(\frac{m_{i-1}}{m_i}\right)^2 + 2\left(\frac{m_{i-1}}{m_i}\right)\right]\Delta V_{I_{k-1}}^2 + \frac{\nu_1}{3C_\infty}\left(\frac{F}{m_i}\right)^2 \frac{\partial T_s\left(\Delta V_i\right)}{\partial \Delta V_i}} \tag{3.2-19}$$

The partial derivative of the transfer time, given by (3.2-7), can be expanded as follows:

$$\frac{\partial T_s\left(\Delta V_i\right)}{\partial \Delta V_i} = 6\pi\mu\left(V_o + \Delta V_i\right)\left[\frac{R}{2\mu - R\left(V_o + \Delta V_i\right)^2}\right]^{5/2} \tag{3.2-20}$$

Equation (3.2-19) gives the useful result that the total velocity impulse ΔV_{i+1} at the end of the kth burn can be calculated from a knowledge of the velocity impulse $\Delta V_{I_{k-1}}$ on the previous segment, the total velocity impulse ΔV_i at the beginning of the burn, and the value of the Lagrange multiplier ν_1. In other words, given the initial velocity impulse and ν_1, an optimal trajectory is

completely specified by (3.2-19). Furthermore, the validity of the use of a first-order approximation for the burn time is ensured by the fact that it is contained in a first order necessary condition.

The N-dimensional parameter problem has thus been reduced to one of two independent variables, ΔV_1 and ν_1. By means of an iterative procedure, ΔV_1 and ν_1 can be chosen such that a unique transfer time can be obtained in exactly N-burns. An optimal N-burn schedule results if the burn time and escape velocity constraints are also satisfied. A desired final energy, i.e., a specified V_∞, can be achieved for a fixed-time transfer by iterating on ΔV_1 until the total impulse on the Nth burn is such that (3.2-14) is satisfied.

The recursion formula (3.2-19) can likewise be used to generate optimal time-open burn schedules by setting the Lagrange multiplier to zero in (3.2-19), i.e.,

$$\Delta V_{i+1} = \Delta V_i + \Delta V_{I_{k-1}} \sqrt{\frac{1}{3}\left[\left(\frac{m_{i-1}}{m_i}\right)^2 + 2\left(\frac{m_{i-1}}{m_i}\right)\right]} \qquad (3.2\text{-}21)$$

This time-open recursion can also be expressed as follows:

$$\frac{\Delta V_{I_k}}{\Delta V_{I_{k-1}}} = \sqrt{\frac{1}{3}\left[\left(\frac{m_{i-1}}{m_i}\right)^2 + 2\left(\frac{m_{i-1}}{m_i}\right)\right]} \qquad (3.2\text{-}22)$$

In other words, for the optimal time-open transfer, the velocity impulses on succeeding burn segments of the equivalent impulsive trajectory are related by a function of the mass ratio between the two segments given by

$$\frac{m_{i-1}}{m_i} = e^{\frac{\Delta V_i - \Delta V_{i-1}}{c}} = e^{\frac{-\Delta V_{I_{k-1}}}{c}} \qquad (3.2\text{-}23)$$

Therefore, for constant thrusting over the burn segment, the equivalent velocity impulses on neighboring segments of a time-open maneuver are related by a function of the velocity impulse on the earlier burn.

Equation (3.2-22) gives a measure of the error in the approximate time-open solution discussed in 3.1. It verifies that, for a negligible mass decrease over each burn, the ratio given by (3.2-23) approaches unity, and neighboring burn segments have equal burn times. For a specific impulse of 800 seconds ($c \approx 2.6 \cdot 10^4$ sec.), the velocity impulses would typically have to be less than 300 fps (which gives a value of 0.99 for (3.2-23)) to yield a valid approximation. Clearly, such small velocity increments would require large values for N and total transfer times out of the range of practical concern.

The following chapter will describe a technique that can be

readily employed to predict optimal time-open and time-fixed multiorbit transfers using the recursive formulation derived above.

CHAPTER IV

ANALYSIS OF A TYPICAL INJECTION MANEUVER

4.1 Time-Open Solution and Determination of Initial Values

The optimal N-burn thrust program for specified values of V_∞ and T_s can be found by iterating on the parameters ΔV_1 and ν_1, where each intermediate impulse schedule $\Delta V_{I_1}, \Delta V_{I_2}, \ldots \Delta V_{I_N}$, is generated by the recursion formula (3.2-19). For the time-open case ($\nu_1 = 0$), the optimal N-burn schedule (for a a specified V_∞) can be computed by iterating on ΔV_1 until the sequence generated by (3.2-21) yields a value for ΔV_N that satisfies the final velocity constraint given by (3.2-14). The impulse schedule obtained corresponds to the optimal time-open N-burn thrust program if the short-burn constraint (3.1-11) is satisfied and if the solution is constrained to exactly N burns by the escape velocity constraint (3.1-12).

If the appropriate value for the initial velocity impulse ΔV_1 is selected, a solution corresponding to the desired value for N can be obtained. However, if a "good" initial value is not selected, a burn schedule corresponding to a different N will be generated and Newton steps will not cause the sequence to converge to the desired N-burn solution. In other words, solutions corresponding to different values of N are independent and self-contained. This

is evident from the nature of the velocity constraint (3.1-12); each N-burn solution is separated from its adjacent (N-1)-burn solution by an (N-1)-burn parabolic escape solution. The independence of N-burn solutions is illustrated in Figures 4.1 and 4.2, which are the results of the simulation described in Appendix C.2. These figures plot, respectively, V_∞ and T_s against the parameter ΔV_1 for the time-open, velocity unconstrained injection maneuver specified by the parameters listed in Appendix B. Not only do these plots demonstrate the independence of N-burn families, but they can be utilized to give excellent starting values for ΔV_1 for a particular N-burn velocity-constrained solution. In other words, if the initial impulse ΔV_1 corresponding to a specified V_∞ and a particular value for N is selected from Figure 4.1, it is guaranteed that (3.2-19) will generate an impulse sequence very close to the desired one, and the Newton iteration will converge in a few steps to the optimal N-burn schedule.

Before discussing the effect of the time constraint (nonzero ν_1), consider the difference in the optimal time-open solution generated by the above method as compared to the approximate time-open solution derived in 3.1. Figures 4.3 and 4.4 present plots of ΔV^* vs. N and T_s vs. N, respectively, for the time-open solution. The locus of solutions corresponding to the approximate time-open case is shown on each figure to provide a simple means of comparing the two methods. The difference in the magnitudes

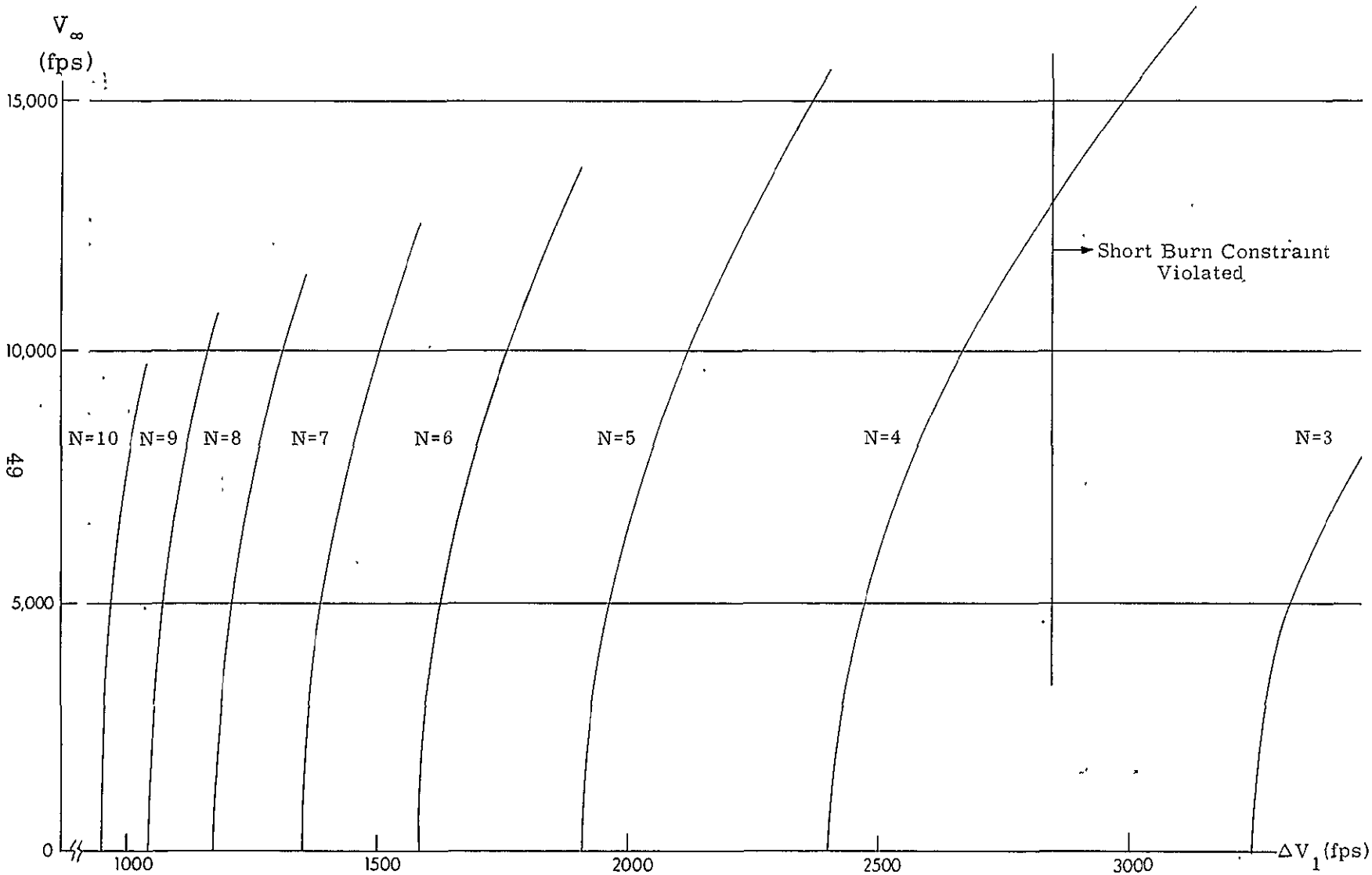

Figure 4.1 V_∞ vs ΔV_1 For Time-Open, Velocity-Unconstrained Maneuver

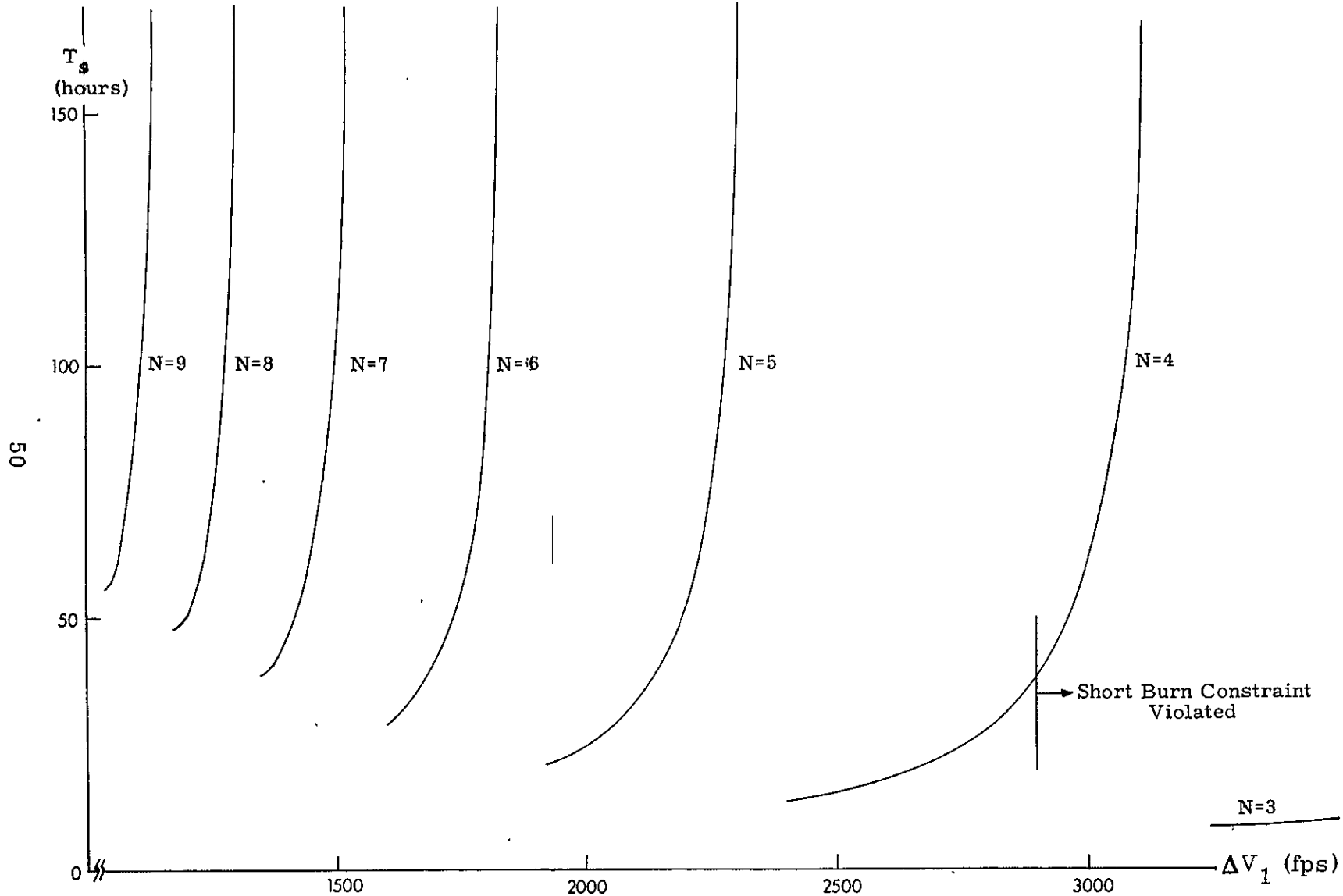

Figure 4.2 T_s vs ΔV_1 For Time-Open, Velocity-Unconstrained Maneuver

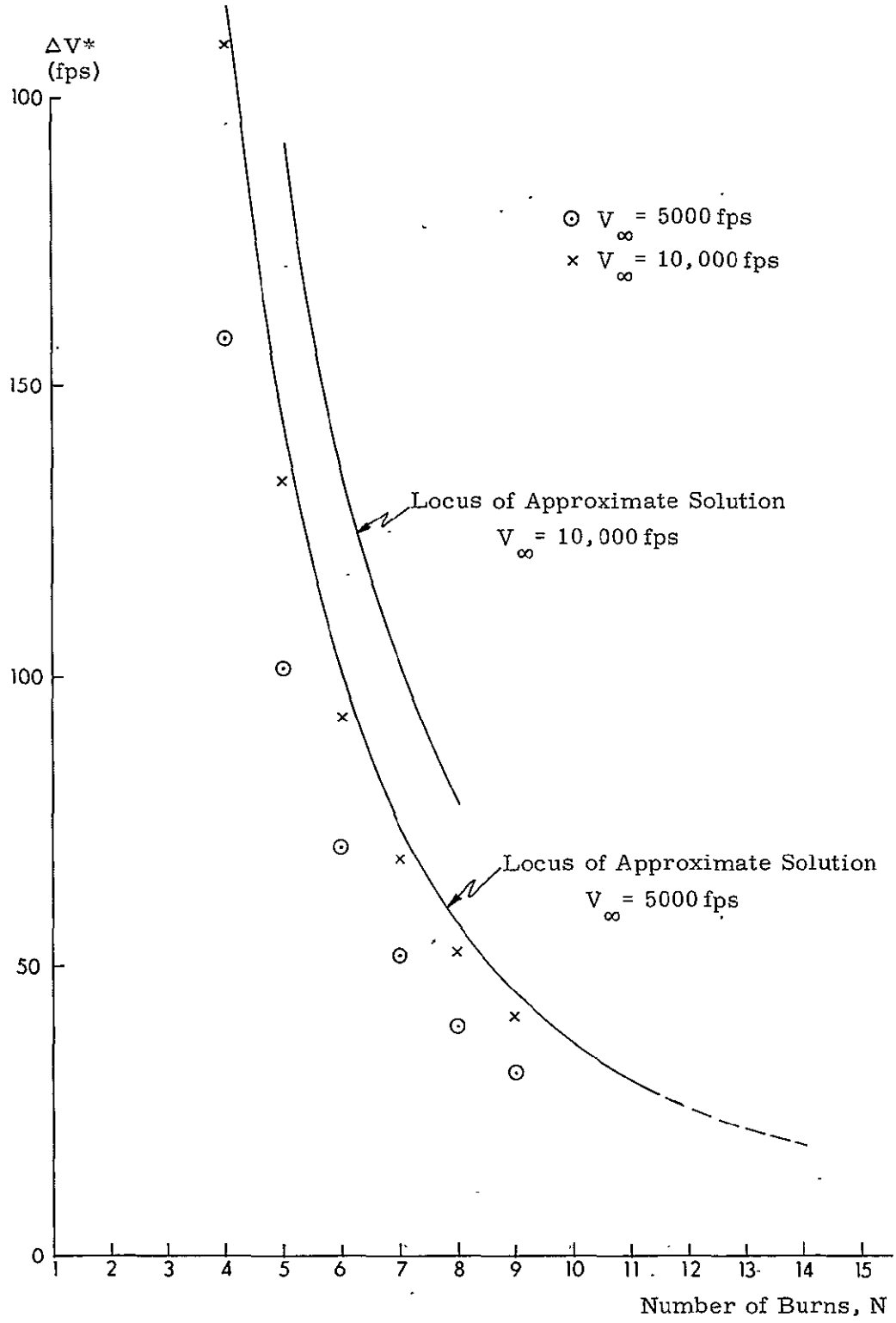

Figure 4.3 ΔV^* vs N For Time-Open Maneuver

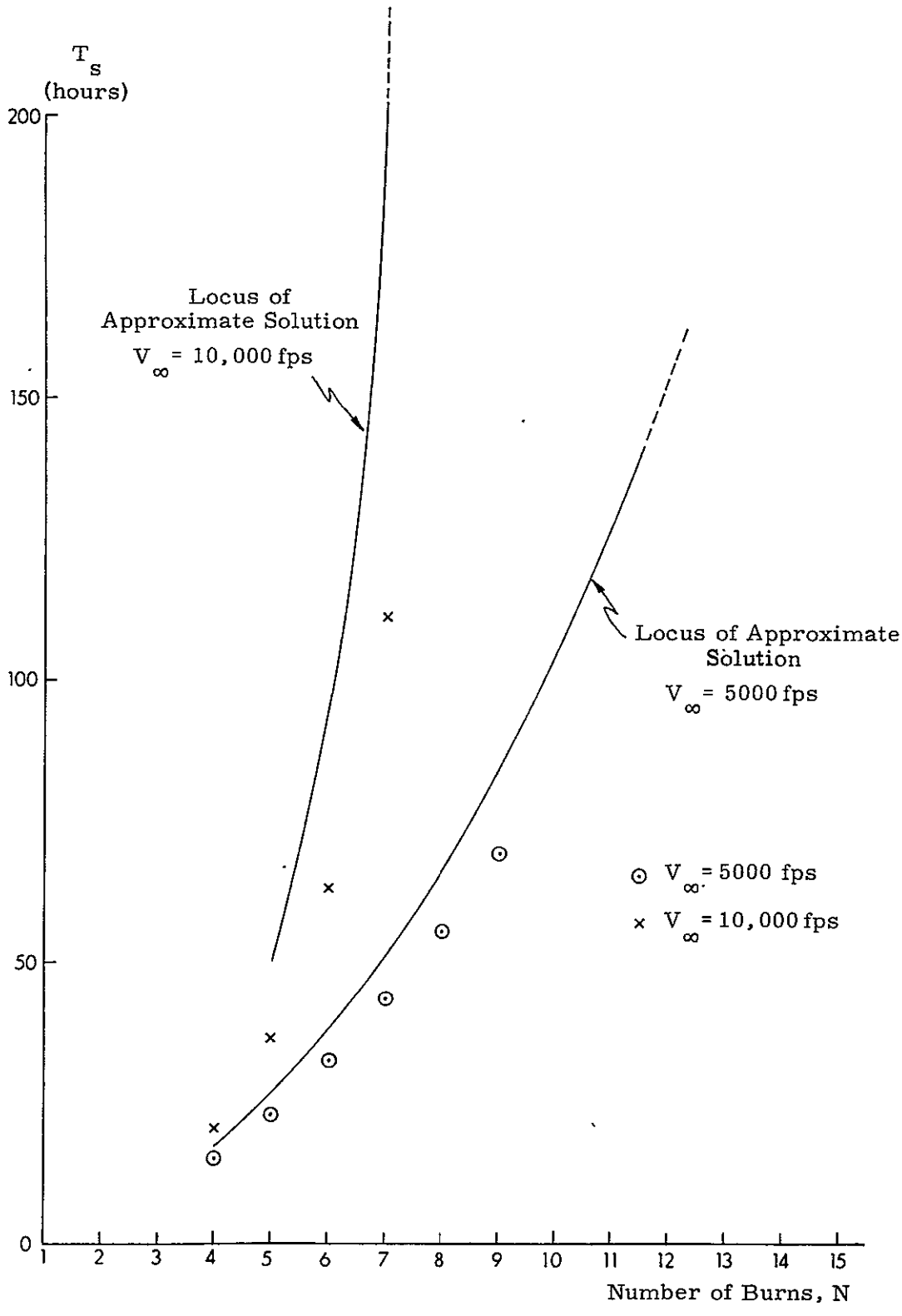

Figure 4.4 T_s vs N For Time-Open Maneuver

between the values given by each method is not surprising, as the exhaust velocity for the powerplant used in the simulation is not particularly large. Nevertheless, these results do show that the recursive solution gives significantly better results for an injection maneuver like the one simulated. Furthermore, contrary to the approximate results given in 3.1, there exists an optimal time-open solution for a final velocity of 15,000 fps corresponding to a 5-burn multiorbit trajectory. Therefore, limits on N for specified values of V_∞ and on V_∞ for specified N's can be obtained from the results of the time-open, velocity-unconstrained simulation. Although solutions only for values of N less than 10 are illustrated in Figures 4.1 - 4.4, the same arguments apply for large values of N. This study will ignore large N solutions, however, as the transfer times and trajectories associated with them are too large for practical purposes.

4.2 Effect of the Time Constraint on the Optimal Burn Schedule

Recalling the necessary condition for a stationary point given by (3.2-8), the Lagrange multiplier ν, which can be written as

$$\nu = \frac{-\partial\phi/\partial\Delta V_i}{\partial\psi/\partial\Delta V_i} \qquad (4.2\text{-}1)$$

represents the sensitivity of changes in cost with respect to changes in the value of the constraint; or, in a plot of ϕ vs. ψ, ν represents

the negative slope of the curve. If the stationary point is a local minimum, values of ψ different from zero must be assigned a positive cost. Hence, ν must be positive for positive values of ψ and negative for negative ψ. This relation is sketched in Figure 4.5

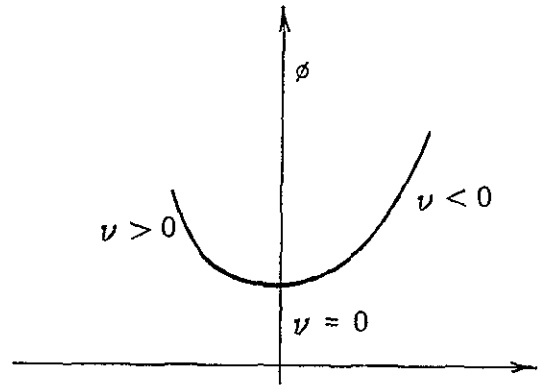

Figure 4.5 ø vs ψ

Applying this argument to the multiorbit-injection problem, it is clear from (3.2-2) that positive ν_1 corresponds to $T_s > T_{sd}$ and negative ν_1 to $T_s < T_{sd}$. Thus, a sketch of the characteristic velocity vs. the time in orbit for a specified V_∞ and a particular value for N should resemble the curve shown in Figure 4.6, where the minimum value of ΔV^* corresponds to the optimal time-open performance penalty and corresponding transfer time.

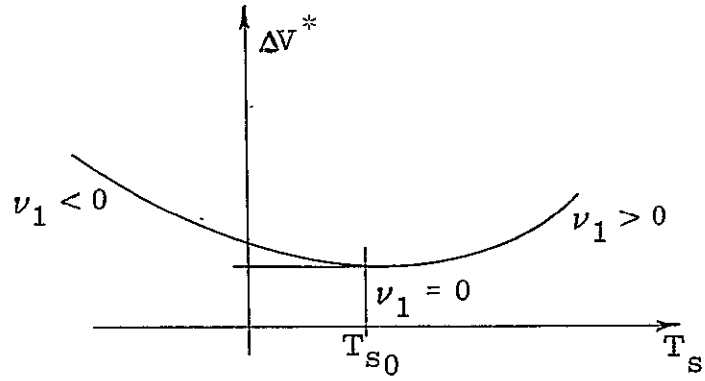

Figure 4.6 Sketch of ΔV^* vs. T_s

A physical interpretation of the effect of the time constraint could be given as follows: For the time-open case ($\nu_1 = 0$), each succeeding burn segment will increase in length by an amount proportional to the velocity-increment ratio given by (3.2-22). Since nonzero values of ν affect the lengths of the ΔV_{I_k} increments on succeeding segments through the second term under the radical in (3.2-19), a positive value for ν_1 tends to make the ΔV_{I_k} increase or successive burn-segments greater; whereas, a negative ν_1 reduces the rate of impulse expansion on successive burn segments. In other words, for $\nu_1 > 0$, (N-1) ΔV_{I_k} segments are "stretched-out" to begin and end at higher absolute periapsis velocities, which correspond to intermediate orbits of greater periods and to a longer overall maneuver time T_s. Similarly, for $\nu_1 < 0$, burn begin times are scheduled at periapse velocities less than those of the corresponding time-open maneuver, and the total injection time T_s is less than that for the time-open case.

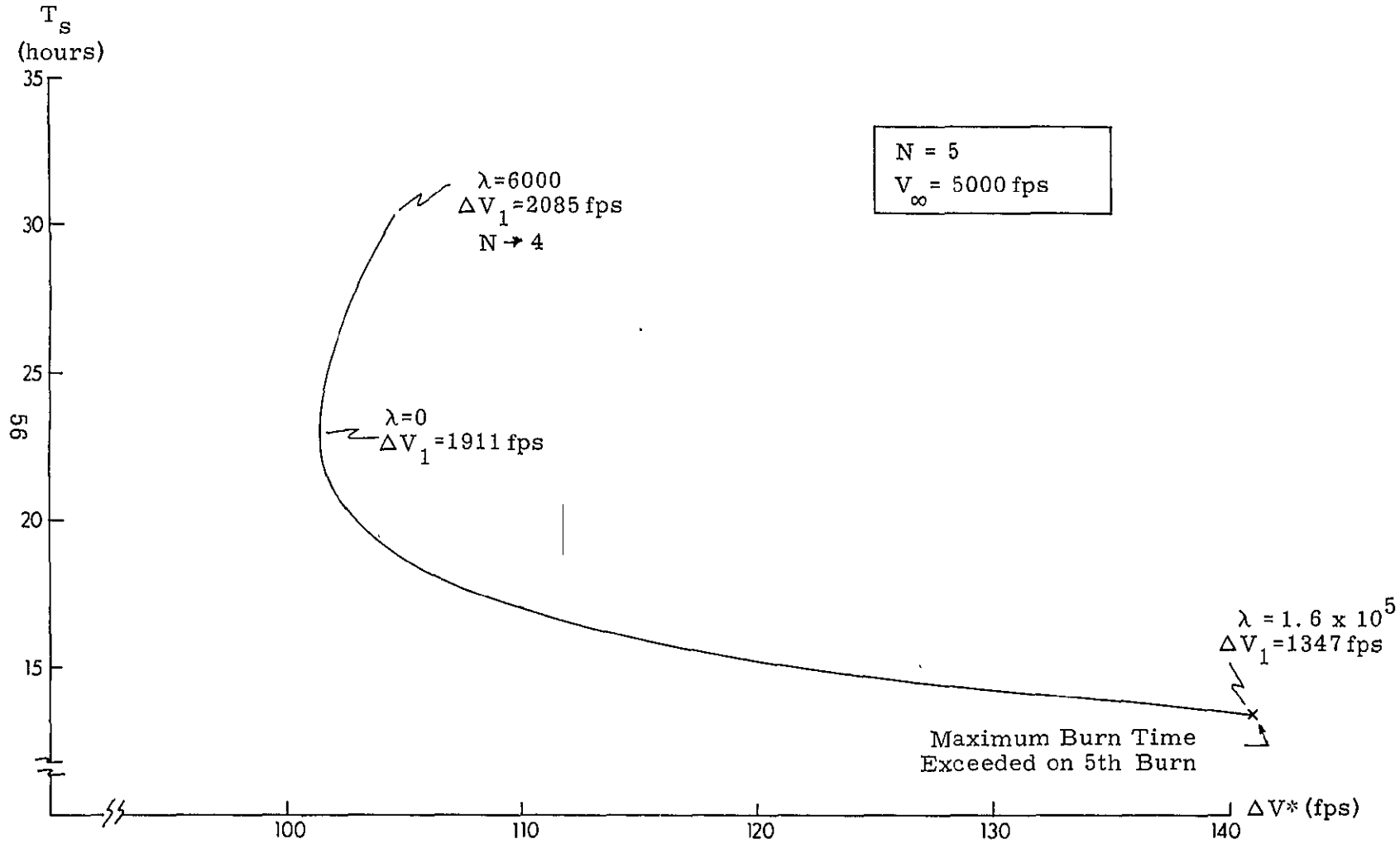

Figure 4.7 T_s vs ΔV^* (N = 5, V_∞ = 5000 fps)

The effects of a time constraint on a typical maneuver (Appendix B) are illustrated by Figures 4.7 and 4.8, which summarize the results of the simulation described in Appendix C.3. Figure 4.7 is a plot of the specified transfer time T_s vs. the characteristic velocity loss ΔV^* for a 5-burn injection to a specified final velocity of 5000 fps. Note that the Lagrange multiplier used in the simulation, λ, is weighted by the constant C_∞ and takes on a sign opposite to that shown in Figure 4.6 (since the constraint is defined with the opposite sign in the simulation). In other words, the Lagrange multiplier shown on Figures 4.6 and 4.7 is given, for convenience, by

$$\lambda = \frac{-\nu_1}{C_\infty} \qquad (4.2\text{-}2)$$

Each point on the curve in Figure 4.7 corresponds to an optimal time-fixed, velocity-constrained burn schedule generated by the recursion formula (3.2-19). Each solution was generated by selecting a value for λ and performing a Newton iteration on the variable ΔV_1 until the final velocity converged to within 5 fps of the desired value. The multiplier λ was varied in the positive and negative direction from $\lambda = 0$. ΔV_1 was initially selected for the time-open case with the aid of Figure 4.1, and each consecutive point on the curve was determined using a greater value for λ and the value of ΔV_1 for which the solution converged on the previous point. The λ recursion was terminated for positive

values when the lower limit on T_s was reached, i. e. when the short burn constraint was exceeded. The recursion on negative λ was terminated when ΔV_1 increased to a value such that the optimal recursion (3.2-19) could not be constrained to 5 burns. The endpoints were not determined precisely, as they are not required in terms of desired results.

The predicted effect of the time constraint on the schedule of velocity impulses is also confirmed by the simulation. The stretching and compressing effect of λ on the impulse sequence is illustrated in Figure 4.8. The Figure compares the thrust program for the optimal time-open 5-burn injection with two corresponding optimal time-fixed transfers, one with a transfer time greater than the time-open maneuver and one with a shorter transfer time. For each of the three cases given, the total required impulse ΔV_I (for an injection to V_∞ = 5000 fps) is divided graphically into 5 burn segments. In each segment the equivalent velocity impulse ΔV_{I_k} and the burn time T_{b_k} are given in units of feet-per-second (fps) and seconds (sec), respectively. The velocity impulse variable ΔV_i can be read from the scale at the bottom of the figure. The semimajor axis (in miles) and the period (in hours) of each intermediate coasting orbit are listed at the end of the appropriate burn segment for each case. The flight path profile for the optimal time-open 5-burn injection corresponds to that shown in Figure 1.

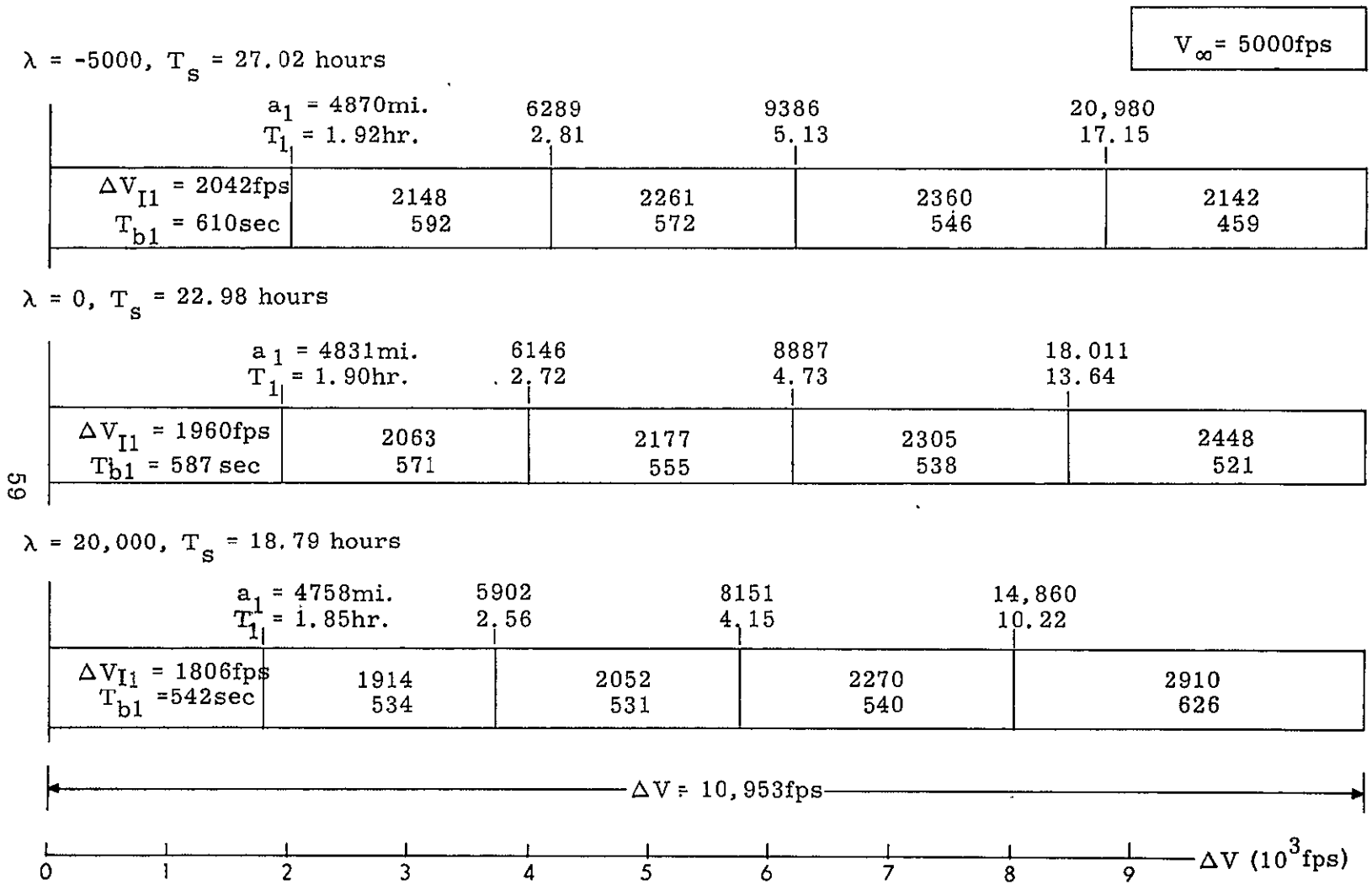

Figure 4.8 Effect of Time Constraint on Burn Schedule

4.3 Determination of the Optimal Time-Fixed Burn Schedule

For a multiorbit injection maneuver of specified final energy, a tradeoff must be made between the transfer time and the performance penalty. Moreover, in order to obtain the optimal burn schedule, maneuvers corresponding to different values of N must be compared. This tradeoff can be readily accomplished with the aid of a plot of T_s vs ΔV^* for various N-burn solutions satisfying a common final energy requirement. For the injection maneuver considered previously, this type of analysis can be carried out with the aid of Figures 4.9 and 4.10, which plot T_s vs ΔV^* for N-burn families corresponding to V_∞ = 5000 fps and V_∞ = 10,000 fps, respectively. Each N-burn curve is generated as described for the 5-burn solution given in Figure 4.7; however, for large values of N, the lower limit on each curve is specified by their intersection with the (N-1)-burn curve rather than by the short-burn constraint. The lower limit on N for a given family of curves is established by the short-burn constraint. N is not taken to its upper limit as these solutions are not of interest.

It is interesting to note the double solutions given by the intersection of curves for larger values of N. The values of T_s and ΔV^* corresponding to one of these points represents two different N-burn optimal transfers; hence, some other criterion must be utilized to select the better solution. In general, the optimal N-burn solution for an injection maneuver of specified V_∞ should

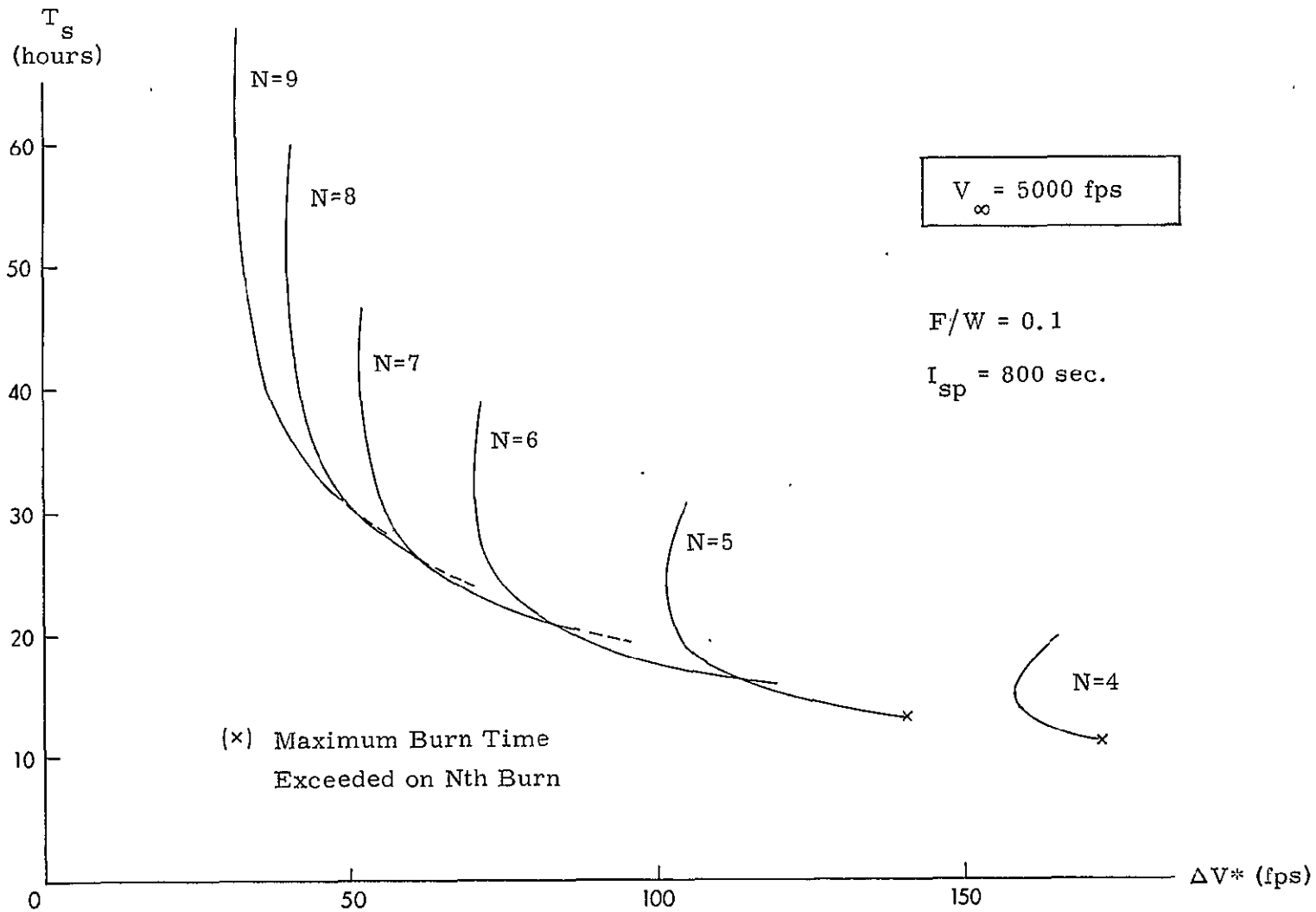

Figure 4.9 T_s vs ΔV^* (V_∞ = 5000 fps)

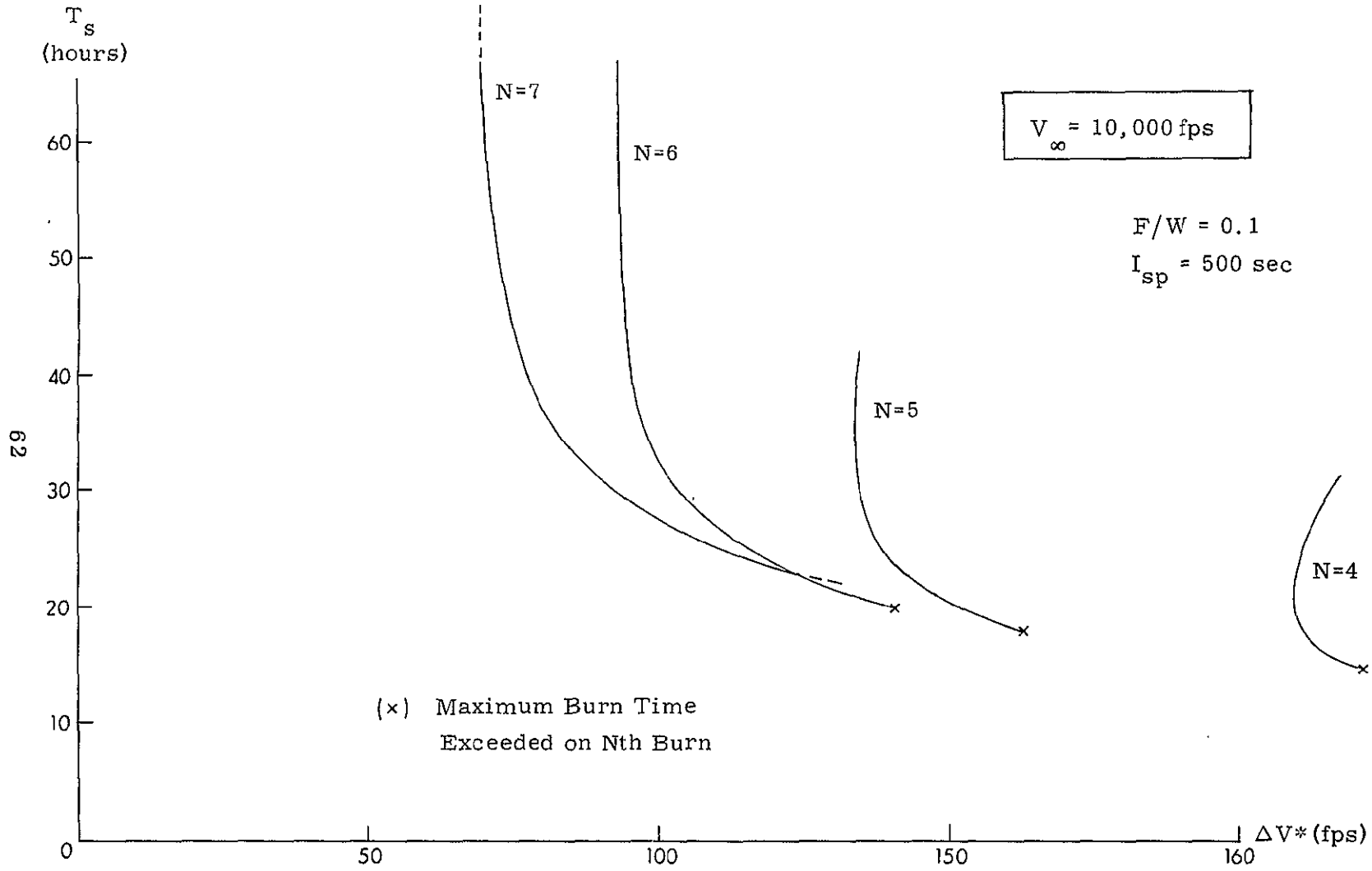

Figure 4.10 T_s vs ΔV^* (V_∞ = 10,000 fps)

lie on the lower edge of the profile described by the family of curves.

If a particular transfer time is specified, the simulation used to generate the T_s vs. ΔV^* curves will not yield the optimal burn schedule in one convergence cycle, since the value of ν_1 that corresponds to a specified T_{sd} is not known. If a particular value of T_s is a critical mission requirement, the optimal N-burn schedule can be obtained by a two-dimensional iteration on the variables ΔV_1 and λ. A two-dimensional Newton iteration which yields a particular time-fixed, velocity-constrained, optimal N-burn schedule is described in Appendix C.4. This technique has several disadvantages, however. First, it requires initial values of ΔV_1 and λ which guarantee that the solution will locally converge to the desired N-burn maneuver. Second, the solution obtained is not a "global" one; hence, it does not guarantee the best thrust program. Therefore, the two-dimensional search method should be used as a secondary routine to obtain a particular fixed-time burn schedule in a local N-burn region. In other words, the time/cost tradeoff should be made from the T_s vs. ΔV^* curves, then the optimal time-fixed solution can be generated by a two-dimensional search routine which utilizes initial values obtained from the one dimensional simulation.

The one-dimensional simulation is not without its difficulties, however. For example, the optimal recursion will not converge

for a parabolic escape maneuver. This tendency can be explained by referring to Figure 4.1, where it can be seen that the slope of each N-burn curve is infinite at $V_\infty = 0$. This implies that the initial value for ΔV_1 must be exact for the solution to converge. Also, for large values of V_∞ and N, the Newton step size must be heavily controlled to constrain the solution to N burns. Fortunately, however, the latter concern is outside the range of interest of this analysis.

4.4 Accuracy of the Solution

In order for the characteristic velocity loss equation to be valid, the burn time must be sufficiently short and the variables r and θ must vary very little during each thrusting phase. A measure of the accuracy of the solution obtained in this analysis is provided by the values taken on by some of the thrust parameters which behave as error quantities. The most obvious measure of the validity of the solution is the burn time. Longer burn times give a less accurate value for the performance penalty, and burn times greater than the upper limit given by (3.1-11) deem the solution invalid as far as this analysis is concerned. Another measure of accuracy is the magnitude of the radial displacement effected during each burn (equation 2.1-4). This displacement, which must be negligible with respect to the radius R of the initial orbit, provides an indirect measure of the span of the thrust arc. These two quantities are tabulated below for various

values of N corresponding to the optimal time-open burn schedules. Also tabulated is the moment correction factor, which was assumed to be unity in the derivation of the recursion formula (3.2-19). For each case, the value of the error quantity represents the "worst case" value for that particular N-burn solution. For the time-open maneuver, the worst case, i. e., the largest, values of T_b and $\underline{d}$ occur on the initial burn segment, whereas, the worst case value for f_k i. e., the one that deviates the most from unity, occurs on the escape segment.

Table 4.1

Worst Case Error Quantities for the Time-Open Maneuver

($F/W = 0.1$, $I_{sp} = 800$ sec.)

	Number of burns N	Burn Time T_{b_1} (sec.)	Radial Displacement $\underline{d}_1$ (miles)	Correction Factor f_N
$V_\infty = 5000$	4	731	18.58	.99976
	5	587	9.37	.99984
	6	490	5.37	.99989
	7	420	3.36	.99992
	8	368	2.24	.99994
	9	328	1.57	.99995
$V_\infty = 10,000$	4	788	22.86	.99972
	5	633	11.52	.99981
	6	528	6.60	.99987
	7	453	4.12	.99990
	8	397	2.75	.99992

For the N-burn time-open maneuver considered in Table 4.1, the burn times stay well within the short-burn constraint but diverge toward $T_{b\,max}$ (837 sec) for small values of N, particularly for larger V_∞. The radial displacement at perigee likewise gets worse for low values of N and large V_∞; however, even for the worst N-burn case shown, the magnitude of the displacement is only 0.56% of the radius of the initial orbit. The values of f_k listed are all within at least 0.01% of unity; thus, the approximation used in the derivation is confirmed by the results of the simulation.

It is also useful to note the variation of these error quantities along the segment of an optimal N-burn multiorbit transfer. For the three cases described in Figure 4.8, the error quantities propagate as shown in Table 4.2. It is interesting to note that for the time-open case ($\lambda = 0$), the error quantities vary little over the trajectory. In fact, the displacement is approximately the same at each perigee. In a sense, one could conclude that these quantities provide a relative measure of the characteristic velocity loss along the trajectory. The only trend indicated by Table 4.2 that is of any concern is the rapid divergence of the error quantities on the last segment of time-fixed maneuver corresponding to positive λ. The values listed on Table 4.2 for this case are within the limits for a good approximation; however, it should be realized that, for some multiorbit injection problems,

Table 4.2

Variation of Error Quantities along as Optimal 5-Burn Multiorbit Trajectory

($F/W = 0.1$, $I_{s_p} = 800$ sec, $V_\infty = 5000$ fps)

	Segment Number k	Burn Time T_{b_k} (sec)	Radial Displacement $\underline{d}_k$ (miles)	Correction Factor f_k
$\lambda = -5000$	1	610	10.55	.99990
	2	592	10.45	.99989
	3	572	10.18	.99987
	4	546	8.42	.99986
	5	454	5.12	.99987
$\lambda = 0$	1	587	9.38	.99990
	2	571	9.37	.99989
	3	555	9.37	.99988
	4	538	9.37	.99987
	5	521	9.36	.99985
$\lambda = 20,000$	1	542	7.43	.99992
	2	534	7.74	.99991
	3	531	8.44	.99989
	4	540	11.19	.99987
	5	626	18.12	.99979

the approximation may degenerate for large values of V_∞ and low values of N.

Other errors associated with the analysis described in this study are the numerical errors inherent in the Newton iteration.

However, for the one-dimensional search utilized, these errors can be made negligible by specifying a more restrictive convergence criterion on the error associated with the final velocity constraint. The analysis has demonstrated that the Newton iteration will converge in a few steps for specified tolerances of less than 0.5 fps on V_∞, i. e., errors less than 0.01% of the magnitude of V_∞. Hence, numerical errors can be made small enough to neglect.

Finally, it should be recalled that there may be a small error in the solution, due to the use of a first-order approximation for the burn time. This type of error can be avoided by finding the impulse schedule that exactly satisfies the first order necessary condition given by (3.2-13). Appendix C.5 outlines an N-dimensional search routine that is designed to do this. The results of this simulation are not presented, as the solution could not be driven to within tolerances that justify its use as a measure of validity of the first-order burn time approximation. Furthermore, an exact solution of the necessary condition may not be justified in light of the nature of the approximation for the characteristic velocity loss.

CHAPTER 5

CONCLUSIONS

This study has presented the followsing results: 1) A simple, closed-form method for calculating gravity losses on multiburn-multiorbit finite thrust trajectories can be developed utilizing Robbins' "impulsive approximation". 2) This approximation can be applied to the multiorbit injection problem for which a simple algorithm can be derived to recursively generate optimal N-burn thrust programs. 3) The recursion algorithm can be used to plot families of time/cost curves for a specified value of the excess hyperbolic velocity, and these curves can be utilized to select initial values from which the optimal N-burn time-fixed injection maneuver can be generated.

The numerical values presented in this study correspond to a particular injection maneuver. It is important to note that the results of the simulations are very sensitive to the selected values of the specific impulse and thrust-to-weight ratio. Clearly, higher values for F/W could be utilized, and the equivalent injection maneuver could be accomplished in fewer burns or with a smaller penalty. In any case, however, due to the nature of the short-burn criterion, the thrust parameters selected will impose restrictions on the final obtainable velocity and the minimum allowable number of burns. In spite of these restrictions, the

method presented in this paper provides a simple and efficient means for predicting optimal thrust programs for N-burn multiorbit injection maneuvers and provides a framework from which optimal burn schedules can be derived for other multiorbit missions.

APPENDIX A

DERIVATION OF CHARACTERISTIC VELOCITY LOSS OVER A SEGMENTED FINITE-THRUST TRAJECTORY*

The differential equations of motion for a vehicle in a vacuum are given by

$$\dot{\underline{r}} = \underline{v}$$

$$\dot{\underline{v}} = \underline{g}(\underline{r}, t) + \underline{a}(t) \qquad \text{(A-1)}$$

where $\underline{r}$ and $\underline{v}$ are, respectively, the position and velocity vectors describing the vehicles motion, $\underline{g}$ is the gravity vector, and $\underline{a}$ is the thrust acceleration vector. If $\underline{r}$ and $\underline{v}$ are perturbed about a nominal trajectory, such that terms of order δr^2 and higher can be neglected, A-1 can be expressed by

$$\delta\dot{\underline{r}} = \delta\underline{v}$$

$$\delta\dot{\underline{v}} = G\delta\underline{r} + \delta\underline{a} \qquad \text{(A-2)}$$

where G is the gravity gradient matrix. If there is no thrusting, i. e., if the vehicle is coasting under the influence of gravity, the

---

* This derivation closely follows that of Robbins [12].

perturbed equations of motion can be written as

$$\begin{bmatrix} \dot{\delta r} \\ \dot{\delta v} \end{bmatrix} = \begin{bmatrix} O & I \\ G & O \end{bmatrix} \begin{bmatrix} \delta r \\ \delta v \end{bmatrix} \tag{A-3}$$

or, in second order form,

$$\ddot{\delta r} = G\,\delta r \tag{A-4}$$

Consider the adjoint system to (A-3) given by

$$\begin{bmatrix} \dot{\mu} \\ \dot{\lambda} \end{bmatrix} = \begin{bmatrix} O & -G \\ -I & O \end{bmatrix} \begin{bmatrix} \mu \\ \lambda \end{bmatrix} \tag{A-5}$$

where μ and λ are (3 x 1) vectors adjoint to r and v, respectively. In second order form, (A-5) becomes

$$\ddot{\lambda} = G\lambda \tag{A-6}$$

Thus, λ, the adjoint to the velocity vector or "primer vector" of Lawden, satisfies the same differential equation as the perturbed position vector.

It can be shown that the primer vector satisfies the identity

$$\lambda \cdot \delta v - \dot{\lambda} \cdot \delta r = \text{constant} \tag{A-7}$$

For non-zero thrust over the time interval (t_o, t_f), it can similarly be shown that

$$\left[\underline{\lambda} \cdot \delta\underline{v} - \dot{\underline{\lambda}} \cdot \delta\underline{r}\right]_{t_o}^{t_f} = \int_{t_o}^{t_f} \underline{\lambda} \cdot \delta\underline{a}\, dt \qquad \text{(A-8)}$$

recognizing that (A-7) takes on a different constant value outisde the burn interval. The variation in the characteristic velocity from its nominal value is given by

$$\delta(\Delta V) = \left[\underline{\lambda} \cdot \delta\underline{v} - \dot{\underline{\lambda}} \cdot \delta\underline{r}\right]_{t_o}^{t_f} + \int_{t_o}^{t_f} (\delta a' - \underline{\lambda} \cdot \delta\underline{a})\, dt \qquad \text{(A-9)}$$

where $\delta a'$ is the variational thrust acceleration over the nominal finite-thrust interval. Assuming that both trajectories start from the same initial state, i.e., $\delta\underline{v}(t_o) = \delta\underline{r}(t_o) = 0$, and that they both satisfy the same final conditions (such that $\delta\underline{r}(t_f)$ and $\delta\underline{v}(t_f)$ are small enough to justify linearity), $\underline{\lambda}(t_f)$ and $\dot{\underline{\lambda}}(t_f)$ can be chosen such that (A-7) is identical to zero over the interval. (A-9) then reduces to

$$\delta(\Delta V) = \int_{t_o}^{t_f} (\delta a' - \underline{\lambda} \cdot \delta\underline{a})\, dt \qquad \text{(A-10)}$$

If the nominal trajectory is optimal, the right hand side of (A-10) must be nonnegative for all perturbations of the acceleration. If optimal steering if utilized, that is, if the acceleration is applied in the direction of the primer vector, $\underline{\lambda} \cdot \delta\underline{a} = |\lambda| \delta a'$,

and (A-10) becomes

$$\delta(\Delta V) = \int_{t_o}^{t_f} (1 - |\underline{\lambda}|)\, \delta a' \, dt \qquad \text{(A-11)}$$

which implies that a necessary condition for an optimal impulsive trajectory is that, at the time the impulse is applied, the magnitude of the primer vector must be unity, and for all other t in the interval, $|\underline{\lambda}| < 1$.

Let ΔV_I be the optimal impulsive velocity on a time unconstrained trajectory, that is, a trajectory on which the time of occurence of the impulse is determined by local optimality with respect to fuel consumption (with the time constraints playing no role except possibly to exclude other local optima). Also, let ΔV_F be the characteristic velocity over a finite thrust trajectory which is not necessarily optimal, but which is close to the optimal impulsive trajectory with respect to position deviations and which satisfies the same end conditions. Then, if $\underline{a}_F$ is the thrust acceleration vector on the finite thrust trajectory and α is the angle between $\underline{a}_F$ and $\underline{\lambda}$, (A-10) can be written as

$$\Delta V_F - \Delta V_I = \int_{t_o}^{t_f} (a_F' - \underline{\lambda} \cdot \underline{a}_F)\, dt$$

$$= \int_{t_o}^{t_f} (1 - |\underline{\lambda}| \cos \alpha)\, a_f \, dt \qquad \text{(A-12)}$$

If t_k are the times of occurence of impulses over a multiburn, segmented trajectory, i. e., one that can be broken up into a series of short burns about local optima and separated by coasting arcs over which $a_F = 0$, the integral (A-12) can be expressed as a sum of integrals, each taken over a short burn period near its respective t_k. Furthermore, cos α can be expanded as

$$\cos \alpha \approx 1 - \frac{1}{2} \alpha^2 \tag{A-13}$$

and the primer vector magnitude can be expanded in a second order Taylor series expansion about t_k, i. e.,

$$\begin{aligned} \left|\underline{\lambda}(t)\right| &= \left|\underline{\lambda}(t_k)\right| + \left|\dot{\underline{\lambda}}(t_k)\right| (t-t_k) + \frac{1}{2} \left|\ddot{\underline{\lambda}}(t_k)\right| (t-t_k)^2 \\ &= 1 + \frac{1}{2} \left|\ddot{\underline{\lambda}}(t_k)\right| (t-t_k)^2 \end{aligned} \tag{A-14}$$

since t_k is at a local maximum. Furthermore, since $\left|\ddot{\underline{\lambda}}(t_k)\right| < 0$ at the local maximum, (A-12) can be expressed as

$$\Delta V_F - \Delta V_I = \sum_{k=1}^{n} \int_{t_{bk}}^{t_{ek}} \left[\frac{1}{2} \alpha^2 - \frac{1}{2} (t-t_k)^2 \left|\ddot{\underline{\lambda}}_k\right| \right] a_F \, dt \tag{A-15}$$

which is valid for a segmented trajectory of n short burns, each of which extend between their respective burn begin times t_{bk} and end times t_{ek}.

If t_{ek} is the centroid time of the thrust acceleration profile on the kth burn, the first moment of the thrust acceleration about its centroid is defined to be zero, i. e.,

$$M_{1k} = \int_{t_{bk}}^{t_{ek}} (t-t_{ck})\, a_F\,(t)\, dt = 0 \qquad \text{(A-16)}$$

and the second moment is given by

$$M_{2k} = \int_{t_{bk}}^{t_{ek}} (t-t_{ck})^2\, a_F\,(t)\, dt \qquad \text{(A-17)}$$

Assuming that α varies approximately linearly during a burn, i. e.,

$$\alpha(t) \approx \alpha_{ck} + (t-t_k)\,\dot{\alpha}_{ck} \qquad \text{(A-18)}$$

and if the burn time is referenced to the centroid time, i. e.,

$$t-t_k = (t-t_{ck}) + (t_{ck}-t_k) \qquad \text{(A-19)}$$

the characteristic velocity loss (A-15) can be written as

$$\Delta V_F - \Delta V_I \approx \frac{1}{2} \sum_{k=1}^{n} \left\{ \left[\alpha_{ck}^{\,2} - \left(t_{ck} - t_k\right)^2 \ddot{\lambda}_k \right] \Delta V_k + \left[\dot{\alpha}_{ck}^{\,2} - \left| \ddot{\underline{\lambda}} \right|_k \right] M_{2k} \right\} dt \qquad \text{(A-20)}$$

where the velocity increments ΔV_k,

$$\Delta V_k = \int_{t_{bk}}^{t_{ek}} a_F(t)\, dt \qquad \text{(A-21)}$$

are given to sufficient accuracy by the impulses of the optimal impulsive trajectory. It can be seen from (A-20) that the optimum choice for the centroid time t_{ck} is the time of occurence of the impulse t_k; and, it can be shown that this choice for t_{ck} is that which also results by requiring the component of position deviation parallel to $\underline{\lambda}(t_k)$ to be approximately zero both before and after the burn. Finally, with optimal timing ($t_{ck} = t_k$) and optimal steering ($\underline{a}_F$ is parallel to $\underline{\lambda}(t)$ such that $\dot{\alpha}_{ck} = \alpha_{ck} = 0$), (A-20) reduces to

$$\Delta V_F - \Delta V_I \approx \frac{1}{2} \sum_{k=1}^{n} -|\ddot{\underline{\lambda}}_k|\, M_{2k} \qquad \text{(A-22)}$$

where the second moment can be accurately approximated as a function of the velocity impulses ΔV_{I_k} on the equivalent impulsive trajectory. By differentiating the identity

$$\underline{\lambda} \cdot \dot{\underline{\lambda}} = |\underline{\lambda}|\, |\dot{\underline{\lambda}}| \qquad \text{(A-23)}$$

(A-6) can be utilized to obtain the relation

$$\underline{\lambda} \cdot \dot{\underline{\lambda}} + \underline{\lambda} \cdot G\underline{\lambda} = |\underline{\lambda}|\, |\ddot{\underline{\lambda}}| + |\dot{\underline{\lambda}}|^2 \qquad \text{(A-24)}$$

Then, since $|\underline{\lambda}| = 1$ and $|\dot{\underline{\lambda}}| = 0$ at t_k, $|\ddot{\underline{\lambda}}_k|$ can be solved for as

$$|\ddot{\underline{\lambda}}|_k = \underline{\lambda} \cdot G\underline{\lambda} + |\dot{\underline{\lambda}}|^2 \qquad \text{(A-25)}$$

Substituting into (A-22), the characteristic velocity loss is given by

$$\Delta V_F - \Delta V_I \approx \frac{1}{2} \sum_{k=1}^{n} \left(-\dot{\underline{\lambda}} \cdot G\underline{\lambda} - |\dot{\underline{\lambda}}|^2 \right) M_{2k} \qquad \text{(A-26)}$$

Therefore, the characteristic velocity loss over a segmented trajectory consisting of n optimally steered and timed finite-burn segments of short duration can be computed in terms of the primer vector solution at the centroid of each burn and the velocity impulses required to effect the equivalent transfers.

APPENDIX B

ORBITAL PARAMETERS AND POWERPLANT DATA

The following data correspond to an injection maneuver from a circular orbit 100 miles above the surface of the earth using a nuclear solid-core rocket consistent with the technology of the late 1970's - early 1980's. These values are incorporated into all the simulations used in this study.

Orbital Parameters:

$\mu = 1.4076 \cdot 10^{16}\ ft^3/sec^2$

$R = 4.0632 \cdot 10^{3}$ mi.

$V_o = 2.561 \cdot 10^{4}$ fps

$T_o = 5.262 \cdot 10^{3}$ sec. = 88 min

$V_E = 3.622 \cdot 10^{4}$ fps

Powerplant Data:

$I_{sp} = 800$ sec.

$F/W = 0.1$

$c = 800\ g = 2.57 \cdot 10^{4}$ fps

Short-burn Constraint:

$T_{b_{max}} = 837.6$ sec.

APPENDIX C

COMPUTER SIMULATIONS

To avoid notational difficulties and unnecessary repitition, a brief summary, rather than a complete program listing, of each simulation is provided in the following sections. The orbital and powerplant data used in each program correspond to the maneuver defined in Appendix B.

C.1 Approximate Time-Open Solution

For a specified value of V_∞ and N, the approximate time-open solution is a completely closed-formed calculation. The simulation repeats itself only for different values of N and V_∞. The total required velocity impulse ΔV_I is calculated from (2.3-4) and the equivalent impulse and the burn time are calculated from (3.1-22). For a given V_∞, the range of N is determined by the upper and lower limits prescribed by the escape velocity and burn time constraints given by (3.1-11) and (3.1-12), respectively. In addition to the segment quantities, this simulation computes the characteristic velocity loss using (3.1-2). The results of the simulation are summarized in Section 3.1.

C.2 Time-Open, Velocity-Unconstrained Simulation

If V_∞ is unspecified and ν_1 is set equal to zero, the curves

given in Figures 4.1 and 4.2 can be generated by selecting various values of ΔV_1 between zero and the approximate time-open $\Delta V_{I_{max}}$ and by performing the recursion given by (3.2-21) until the escape velocity is exceeded. The value for the index is set equal to N on this step, and V_∞ is computed from (3.2-14). Hence, the array ΔV_1, ΔV_2, ... ΔV_N is defined, and all orbital quantities (m_i, a_i, T_i) and burn segment quantities (ΔV_{I_k}, T_{b_k}, d_k, f_k) can be calculated using the equations given in Chapters 2 and 3.

C.3 Time-Fixed Recursive Solution for Specified V_∞

If V_∞ and λ are specified and if a good initial value for ΔV_1 is selected (from Figure 4.1), such that the value of N given by the recursion (3.2-19) and the escape velocity constraint (3.1-12) corresponds to the desired value, a one-dimensional Newton iteration on ΔV_1 can be effected such that the final velocity given by (3.1-2) will converge to the desired value in a few steps. The classical one-dimensional Newton step is defined as

$$\Delta x = -\frac{f(x)}{f'(x)} \qquad \text{(C.3-1)}$$

where f(x) is the value of the function that is to be driven to zero by proper choice of the variables x and $f'(x)$ is the derivative of that function with respect to x.

In this simulation f(x) corresponds to the final velocity constraint, given by

$$f(x) = \psi(\Delta V_1) = V_{\infty d} - V_\infty \qquad \text{(C.3-2)}$$

and f (x) is given by

$$f\,(x) = \frac{\partial \psi(\Delta V_1)}{\partial \Delta V_1} = \frac{-\partial V_\infty}{\partial \Delta V_1} \qquad \text{(C.3-3)}$$

The derivative is computed numerically by a balanced difference, i. e.,

$$\frac{dV_\infty}{d\Delta V_1} \approx \frac{V_\infty (\Delta V_1 + \delta) - V_\infty (\Delta V_1 - \delta)}{2\,\delta} \qquad \text{(C.3-4)}$$

where δ is a small increment, specified in this simulation as

$$\delta = .01\ \Delta V_1$$

Subsequent values of ΔV_1 in the iteration are computed as follows:

$$\delta(\Delta V_1)_{k+1} = (\Delta V_1)_k - \frac{\psi(\Delta V_1)_k}{\frac{\partial \psi(\Delta V_1)_k}{\partial (\Delta V_1)_k}} \qquad \text{(C.3-5)}$$

The iteration is continued until the velocity constraint (C.3-2) has converged to within some specified value of zero. The convergence criterion used in the simulation is given by

$$\psi(\Delta V_1) < 5.0 \text{ fps} \qquad \text{(C.3-6)}$$

This criterion gives good results as well as convergence in two or three steps. To assure convergence the step size has to be controlled in the region of the solution. The control used in this simulation is simply a halving of the kth step size $\delta(\Delta V_1)_k$ if the error, given by (C.3-2), is not decreased on the kth step.

When the iteration converges to the optimal impulse sequence, the orbital and segment quantities as well as T_s and ΔV^* are computed, as in the velocity unconstrained simulation. The iteration cycle corresponds to particular values of V_∞, N, and λ and represents one cycle of the iteration on λ described in Section 4.2. When a sufficient number of cycles are run to plot a complete T_s vs ΔV^* curve, new initial values for ΔV_1 are read in and another N-burn family is simulated. The results of this simulation are summarized in Figures 4.9 and 4.10 for two values of V_∞. All of the orbital and segment quantities given in Chapter 4 for the 5-burn maneuver are computed by this simulation.

C.4 Two-Dimensional Search for Specified V_∞ and T_s

If the transfer time T_s is specified along with V_∞, the optimal N-burn schedule can be obtained by selecting the proper starting values and iterating consecutively on the variables ΔV_1 and λ until the velocity and time constants are satisfied. The iteration follows that described in C.3; the two dimensional Newton step is defined below.

Let the generalized 2-dimensional constraint $\underline{\psi}$ have components ψ_1 and ψ_2, where ψ_1 is the velocity constraint given by C.3-2 and ψ_2 is the time constraint given by

$$\psi_2(\lambda) = T_{sd} - T_s \qquad \text{(C.4-1)}$$

The step $\delta(\Delta V_1)$, $\delta\lambda$ that drives (C.3-2) and C.4-1) simultaneously to zero is given by the solution to the following equations:

$$\begin{aligned} d\psi_1 &= \frac{\partial\psi_1}{\partial\Delta V_1}\,\delta(\Delta V_1) + \frac{\partial\psi_2}{\partial\lambda}\,\delta(\lambda) = -\psi_1 \\ d\psi_2 &= \frac{\partial\psi_2}{\partial\Delta V_1}\,\delta(\Delta V_1) + \frac{\partial\psi_2}{\partial\lambda}\,\delta(\lambda) = -\psi_2 \end{aligned} \qquad \text{(C.4-2)}$$

If the variables are renamed as follows :

$$\psi_1 = F \qquad \psi_2 = G$$

$$\Delta V_1 = x \qquad \lambda = y$$

$$\frac{\partial \psi_1}{\partial \Delta V_1} = F_x \qquad \frac{\partial \psi_2}{\partial \Delta V_1} = G_x$$

$$\frac{\partial \psi_1}{\partial \lambda} = F_y \qquad \frac{\partial \psi_2}{\partial \lambda} = G_y$$

Cramers' Rule yields the following solution to C. 4-2:

$$\delta x = \frac{G F_y - F G_y}{F_x G_y - F_y G_x} = \delta(\Delta V_1) \qquad \text{(C. 4-2)}$$

$$\delta y = \frac{F G_x - G F_x}{F_x G_y - F_y G_x} = \delta(\lambda)$$

Step size control on both components of the step is employed as in C. 3. As mentioned in Chapter 4, this simulation is very sensitive to the initial values selected and it does not guarantee convergence unless the iteration is initiated in the region of the stationary point. Good initial values can be selected from the T_s vs ΔV^* curves obtained from the 1-dimensional iteration C. 3, but since these curves supply the information needed, the simulation outlined here is only useful as a refinement on data

which must be interpolated from the T_s vs. ΔV^* curves.

C.5 N-Dimensional Search for Exact Solution

Given an initial set of values $\{\Delta V_1, \Delta V_2, \ldots \Delta V_N\}$ (as obtained from the simulation C.3), an N-dimensional step $\delta(\Delta V_1)$, $\delta(\Delta V_2)$, ... $\delta(\Delta V_N)$ can be taken such that the new ΔV array will be driven toward that set of values which satisfy the first order necessary condition (3.2-13) and the velocity constraint (3.2-14). In other words, for i = 1, 2, ... (N-1), ΔV_i must satisfy (3.2-13), and ΔV_N must satisfy (3.2-14). Therefore, the N constraint equations which must be satisfied are given by

$$
\begin{aligned}
F_1\left(\Delta V_0, \Delta V_1, \Delta V_2\right) &= 0 \\
F_2\left(\Delta V_1, \Delta V_2, \Delta V_3\right) &= 0 \\
&\cdot \\
&\cdot \\
&\cdot \\
F_{N-1}\left(\Delta V_{N-2}, \Delta V_{N-1}, \Delta V_N\right) &= 0 \\
G\left(\Delta V_N\right) &= 0 \qquad \text{(C.5-1)}
\end{aligned}
$$

where ΔV_0 is zero.

The N-dimensional Newton step $\underline{\delta(\Delta V)}$ that drives these constraints to zero is given by the solution to the following set of

equations:

$$dF_1 = \frac{\partial F_1}{\partial \Delta V_1}\delta(\Delta V_1) + \frac{\partial F_1}{\partial \Delta V_2}\delta(\Delta V_2) + \ldots + \frac{\partial F_1}{\partial \Delta V_N}\delta(\Delta V_N) = -F_1$$

$$dF_2 = \frac{\partial F_2}{\partial \Delta V_1}\delta(\Delta V_1) + \frac{\partial F_2}{\partial \Delta V_2}\delta(\Delta V_2) + \ldots + \frac{\partial F_2}{\partial \Delta V_N}\delta(\Delta V_N) = -F_2$$

$$\vdots$$

$$dF_{N-1} = \frac{\partial F_{N-1}}{\partial \Delta V_1}\delta(\Delta V_1) + \frac{\partial F_{N-1}}{\partial \Delta V_2}\delta(\Delta V_2) + \ldots + \frac{\partial F_{N-1}}{\partial \Delta V_N}\delta(\Delta V_N) = -F_{N-1}$$

$$dG = \frac{\partial G}{\partial \Delta V_1}\delta(\Delta V_1) + \frac{\partial G}{\partial \Delta V_2}\delta(\Delta V_2) + \ldots + \frac{\partial G}{\partial \Delta V_N}\delta(\Delta V_N) = -G \qquad \text{(C.5-2)}$$

Since G is a function of ΔV_N only,

$$\frac{\partial G}{\partial \Delta V_i} = \begin{cases} 0 & i \neq N \\ 1 & i = N \end{cases} \qquad \text{(C.5-3)}$$

and since F_i is a function of only ΔV_{i-1}, ΔV_i, and ΔV_{i+1},

$$\frac{\partial F_i}{\partial \Delta V_i} = 0 \quad \text{For } j \neq (i-1),\ i,\ (i+1) \qquad \text{(C.5-4)}$$

The step components $\delta(\Delta V_i)$ can be solved for from (C.5-2) using Cramer's Rule; but, before giving the result, define the

vectors

$$\underline{x} = \left\{\Delta V_1,\ \Delta V_2,\ \ldots\ \Delta V_N\right\}$$

$$\delta\underline{x} = \left\{\delta\left(\Delta V_1\right),\ \delta\left(\Delta V_2\right),\ \ldots\ \delta\left(\Delta V_N\right)\right\}$$

$$\underline{\psi} = \left\{F_1,\ F_2,\ \ldots\ F_{N-1},\ G\right\} \qquad \text{(C.5-5)}$$

where $\underline{x}$ is the vector of parameters ΔV_i, $\delta\underline{x}$ is the Newton step vector, and $\underline{\psi}$ is the generalized constraint vector. Hence, the N-dimensional Newton step is found from the solution to the following equation:

$$D\delta\underline{x} = -\underline{\psi} \qquad \text{(C.5-6)}$$

where D is the matrix of partial derivatives given by

$$D = \begin{bmatrix} F_{11} & F_{12} & \cdots & F_{1N} \\ F_{21} & F_{22} & \cdots & F_{2N} \\ \vdots & & & \\ F_{(N-1)1} & F_{(N-1)2} & \cdots & F_{(N-1)N} \\ 0 & 0 & \ldots & 1 \end{bmatrix} \qquad \text{(C.5-7)}$$

such that $$[D]_{ij} = \frac{\partial \psi_i}{\partial \Delta V_j}.$$

The new value for the parameter vector is computed from

$$\underline{x}_{k+1} = \underline{x}_k - \delta \underline{x}_k \qquad \text{(C.5-8)}$$

The Newton step increment is given by Cramer's Rule as

$$\delta \underline{x}_k = \frac{\underline{\underline{N}}}{D}$$

where each element N_j of the n-dimensional numerator vector $\underline{N}$ is the determinate of the matrix of partials D with its jth column replaced by the constraint vector $\underline{\psi}$.

The partial derivatives are computed numerically by differencing, and the step size control utilized previously is applied to each component of the step increment vector. The analysis was terminated when it became evident that a more sophisticated step size control was necessary to make the N-dimensional constraint converge to within strict tolerances.

REFERENCES

1. Battin, R. H., Astronautical Guidance, McGraw-Hill, 1964.

2. Edelbaum, T. N., "Calculation of Interplanetary Trajectories in the Vicinity of Planets," United Aircraft Research Labs Paper, Feb., 1966.

3. Edelbaum, T. N., "Optimal Guidance From Hyperbolic to Circular Orbits," Reprint from Advanced Problems and Methods for Space Flight Optimization, 1969.

4. Edelbaum, T. N., "Theory of Maxima and Minima," from Optimization Techniques, ed. George Leitmann, Academic Press, 1962.

5. Funk, J and McAdoo, S. F., "Application of Nuclear Solid-Core Rockets to Interplanetary Orbital Launch by Multiorbit Injection," AIAA Paper No. 69-535, 1970.

6. Funk, J., and McAdoo, S. F., "Switching Logic and Steering Equations for Multiple-burn Earth Escape Maneuvers," Institute of Navigation, 1969, National Space Meeting.

7. Gobetz, F. W. and Doll, J. R., "A Survey of Impulsive Trajectories," AIAA Journal, Vol. 7, No. 5, May, 1969.

8. Henrici, P., Elements of Numerical Analysis, John Wiley and Sons, 1964.

9. Johnson, P. G. and Rom, F. E., "Perigee Propulsion for Orbital Launch of Nuclear Rockets," NASA Technical Report R-140, 1962.

10. Lawden, D. F., Optimal Trajectories for Space Navigation, Butterworths (London), 1963.

11. Lion, P. M., "A Primer on the Primer," Second Compilation of Papers on Trajectory Analysis and Guidance Theory, NASA PM-67-21, Jan., 1968.

12. Robbins, Howard M., "An Analytical Study of the Impulsive Approximation," AIAA Journal, Vol. 4, No. 8, August, 1966.

13. Robbins, H. M., "Optimal Steering for Required Velocity Guidance," Navigation, Vol. 12, No. 4, Winter, '65-'66.